Electronic Supplementary Information

Supramolecular Assembly of DNA-Constructed Vesicles

Simon Rothenbühler,[a] Ioan Iacovache,[b] Simon M. Langenegger,[a] Benoît Zuber*[b] and Robert Häner*[a]

[a] Department of Chemistry and Biochemistry, University of Bern, Freiestrasse 3, CH – 3012 Bern, Switzerland

[b] Institute of Anatomy, University of Bern, Baltzerstrasse 2, CH – 3012 Bern, Switzerland

Table of contents

1. Abbreviations

AFM	Atomic force microscopy
APTES	(3-Aminopropyl)triethoxysilane
BOP	(Benzotriazol-1-yloxy)tris(dimethylamino)phosphonium hexafluorophosphate
CEP-Cl	2-Cyanoethyl *N*,*N*-diisopropylchlorophosphoramidite
DCM	Dichloromethane
DIPA	Diisopropylamine
DMAP	*N*,*N*-Dimethylpyridin-4-amine
DMT-Cl	4,4'-Dimethoxytrityl chloride
Et_3N	Triethylamine
EtOAc	Ethyl acetate
^{i}PrOH	Propan-2-ol
LCAA-CPG	Long chain alkylamine controlled pore glass
MeOH	Methanol
RM	Reaction mixture
rt.	Room temperature
THF	Tetrahydrofuran
TLC	Thin-layer chromatography
TPE	Tetraphenylethylene

2. General methods

All reagents and solvents were purchased from commercial suppliers and used without further purification. All reactions were accomplished under argon atmosphere using anhydrous solvents. Oligonucleotides **C**, **D**, **E**, and **F** were purchased from Microsynth (Switzerland). TLCs were conducted on silica gel SIL G UV_{254} glass plates (Macherey-Nagel). Flash column chromatography was performed on Sigma Aldrich silica gel, pore size 60 Å, 230-400 mesh particle size. Water was used from a Milli-Q system. NMR spectra were obtained on a Bruker Avance III HD (400 MHz) spectrometer at 298 K (unless noted otherwise) from the Analytical Research and Services (ARS) of the University of Bern, Switzerland. Mass spectra were obtained on a Thermo Fisher LTQ Orbitrap XL using Nano Electrospray Ionization (NSI) from the ARS. Spectroscopic data were measured from at least five minutes thermally equilibrated samples at the corresponding temperature. UV-vis spectra were recorded on an Agilent Cary 100 spectrophotometer using quartz cuvettes with an optical path of 1 cm. Fluorescence spectra were collected on a Cary Eclipse fluorescence spectrophotometer using an excitation slit of 2.5 nm and an emission slit of 5 nm (unless noted otherwise). Supramolecular assembly proceeded *via* thermal disassembly and reassembly: the sample solution was heated to 75 °C, followed by a controlled cooling of 0.5 °C/min to 20 °C in a Cary Eclipse fluorescence spectrophotometer equipped with a Peltier thermostat. Samples for cryo-electron microscopy were plunge frozen using the FEI Vitrobot Mach 4 at room temperature and 100% humidity. In brief, quantifoil 2/1 copper grids were glow discharged (10 mA for 20 seconds). 3 µL of the sample were pipetted on the girds and blotted for 3 seconds before plunging into liquid ethane/propane mix. Sample grids were stored in liquid nitrogen. Images were acquired using a Gatan 626 cryo holder on a Falcon III equipped FEI Tecnai F20 in nanoprobe mode. Due to the nature of the sample, acquisition settings had to be adjusted for a low total electron dose (less than 20 $e^-/Å^2$) using EPU software. Distance measurements were done in Fiji[1–3] using the multi-point tool to set marks. After the read-out of the x- and y-values, the distances between the marks were calculated. The reported distances are mean values with the corresponding standard deviation. AFM experiments were conducted on a Nanosurf FlexAFM instrument in tapping mode under ambient conditions. AFM samples were prepared on APTES-modified mica sheets (Glimmer "V1", 20 mm x 20 mm, G250-7, Plano GmbH) according to published procedures.[4] Therefore, mica sheets were freshly cleaved and mounted with tape on top of a desiccator (3 L), before the desiccator was purged with argon. APTES (30 µL) was pipetted into an Eppendorf tube cap and Hünig's base (10 µL) was added into a second cap. Both Eppendorf tube caps were placed at the bottom of the desiccator below the mica sheets, then the desiccator was closed. The chemicals were allowed to evaporate for 2 h, before the caps were removed, and the desiccator was flushed with argon. The mica sheets were left for one day in the desiccator to cure. Afterwards, the corresponding sample solution (20 µL) was pipetted onto the APTES-modified mica sheet. After an adsorption time of 10 min, the mica sheet was rinsed with Milli-Q water (2 mL), then dried under a stream of argon. Dialysis buttons (HR3-332, Hampton research) and regenerated cellulose dialysis tubing (Spectra/Por 4™, 12–14 kDa MWCO, 132 700) was utilized for dialysis. The samples were dialyzed against 200 mL of 10 mM sodium phosphate pH 7.2, 0.1 mM spermine · 4 HCl dialysate buffer for at least 3 h to remove the ethanol (< 0.5 vol%). The successful removal of the ethanol fraction was confirmed by measuring the refractive index of a control, that was treated identically to the respective sample and compared against a calibration curve. Refractive index measurements were conducted on a Reichert Abbe Mark III refractometer in the automatic temperature correction mode.

3. Organic synthesis

The synthesis of *E*-TPE phosphoramidite **5** was adapted from published procedures (Scheme S1).[5]

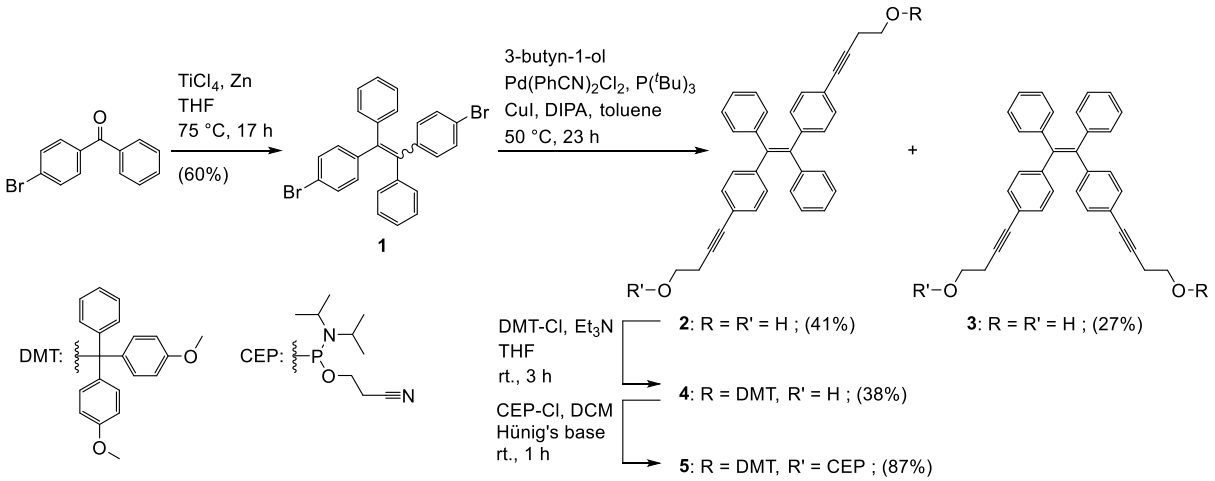

Scheme S1: Synthesis of *E*-TPE phosphoramidite **5**.

1,2-Bis(4-bromophenyl)-1,2-diphenylethene (1)

4-Bromobenzophenone (6.53 g, 25.01 mmol) and Zn dust powder (4.92 g, 75.25 mmol) were suspended in THF (150 mL). The grey suspension was cooled to 0 °C, before $TiCl_4$ (4.1 mL, 37.40 mmol) was added slowly. After the RM was warmed to rt., it was refluxed at 77 °C for 15 h. TLC (DCM) showed disappearance of starting material. The RM was cooled to rt., before aq. 10% K_2CO_3 (125 mL) was added. The RM was filtered through celite and the filter cake was washed thoroughly with THF, followed by DCM. The yellow filtrate was extracted three times with DCM (3x80 mL). The combined organic layers were washed once with brine (100 mL), dried over $MgSO_4$, filtered, and concentrated *in vacuo*. The resulting yellow, oily residue was dissolved in DCM (4 mL), then precipitated into cold MeOH (625 mL) while stirring. The forming white solid was filtered off and washed with cold MeOH. An *E*-/*Z*- mixture of compound **1** was isolated as a white powder (3.65 g, 7.45 mmol, 60%). R_f = 0.88 (DCM); ^{1}H NMR (400 MHz, DCM-d_2) δ 7.30–7.21 (m, 4H), 7.17–7.10 (m, 6H), 7.04–6.99 (m, 4H), 6.93–6.87 (m, 4H); ^{13}C NMR (101 MHz, DCM-d_2) δ 143.57, 143.44, 143.12, 143.00, 140.97, 133.44, 131.69, 131.58, 131.39, 128.53, 128.35, 127.47, 127.35, 121.20, 121.06; HRMS-NSI (*m/z*): $[M]^+$ calcd for $C_{26}H_{18}Br_2$, 487.9770; found, 487.9762.

(*E*)-4,4'-((1,2-diphenylethene-1,2-diyl)bis(4,1-phenylene))bis(but-3-yn-1-ol) (2) and (*Z*)-4,4'-((1,2-diphenylethene-1,2-diyl)bis(4,1-phenylene))bis(but-3-yn-1-ol) (3)

The *E*-/*Z*- mixture of starting material **1** (1.084 g, 2.21 mmol), $Pd(PhCN)_2Cl_2$ (54 mg, 6 mol%), and CuI (30 mg, 6 mol%) were dissolved in toluene (22.5 mL) and DIPA (5.6 mL). A 1 M solution of $P(^tBu)_3$ in toluene (0.27 mL, 12 mol%) was added carefully, followed by 3-butyn-1-ol (0.25 mL, 3.3 mmol). The RM was heated to 50 °C and stirred at this temperature for 5 h. 3-Butyn-1-ol (0.17 mL, 2.3 mmol) was added and the RM was stirred at 50 °C for further 18 h. TLC (DCM/MeOH 99:1) showed disappearance of starting material **1**, the appearance

of mono-reacted byproduct and the desired products **2** and **3**. The dark brown RM was cooled to rt., before it was diluted with toluene (10 mL) and filtered through celite. The grey filter cake was washed with toluene (20 mL), followed by DCM (50 mL). The filtrate was further diluted with DCM (100 mL). The organic layer was washed once with aq. 10% citric acid (150 mL), once with aq. sat. $NaHCO_3$ (200 mL), once with brine (200 mL), dried over $MgSO_4$, filtered, and concentrated *in vacuo*. The residue was purified by flash column chromatography on silica gel (DCM/toluene/^{i}PrOH 95.5:4:0.5 → 70:20:10) to yield a preliminary separation of product **2** and **3**, respectively. Crude product **2** (600 mg) was repurified by flash column chromatography on silica gel (DCM/MeOH 99.9:0.1 → 98:2). Product **2** was afforded as a yellowish foam (424 mg, 0.90 mmol, 41%). R_f = 0.24 (DCM/MeOH 99:1); ^{1}H NMR (333 K, 400 MHz, CD_3CN) δ 7.18–7.11 (m, 10H), 7.08–7.03 (m, 4H), 7.01–6.95 (m, 4H), 3.66 (q, *J* = 6.4 Hz, 4H), 2.74 (t, *J* = 6.0 Hz, 2H), 2.56 (t, *J* = 6.5 Hz, 4H); ^{13}C NMR (333 K, 101 MHz, CD_3CN) δ 144.50, 144.41, 142.41, 132.20, 132.16, 131.98, 129.10, 128.02, 123.24, 89.43, 82.32, 61.76, 24.59; HRMS-NSI (*m/z*): $[M]^+$ calcd for $C_{34}H_{28}O_2$, 468.2084; found, 468.2083. Crude product **3** (310 mg) was repurified by flash column chromatography on silica gel (DCM/MeOH 99.5:0.5 → 97:3). Product **3** was isolated as a yellowish foam (281 mg, 0.60 mmol, 27%). R_f = 0.10 (DCM/MeOH 99:1); ^{1}H NMR (333 K, 400 MHz, CD_3CN) δ 7.18–7.11 (m, 10H), 7.08–7.03 (m, 4H), 7.00–6.96 (m, 4H), 3.67 (q, *J* = 6.4 Hz, 4H), 2.76 (t, *J* = 6.0 Hz, 2H), 2.57 (t, *J* = 6.5 Hz, 4H); ^{13}C NMR (333 K, 101 MHz, CD_3CN) δ 144.47, 144.40, 142.40, 132.21, 132.13, 132.06, 129.01, 127.94, 123.32, 89.49, 82.34, 61.76, 24.61; HRMS-ESI (*m/z*): $[M]^+$ calcd for $C_{34}H_{28}O_2$, 468.2084; found, 468.2082.

(*E*)-4-(4-(2-(4-(4-(bis(4-methoxyphenyl)(phenyl)methoxy)but-1-yn-1-yl)phenyl)-1,2diphenylvinyl)phenyl) but-3-yn-1-ol (4)

Starting material **2** (798 mg, 1.70 mmol) was dissolved in THF (20 mL) and Et_3N (5 mL). DMT-Cl (289 mg, 0.85 mmol) was added to the clear, yellow solution at rt. After 20 min, DMT-Cl (288 mg, 0.85 mmol) was added. The RM was stirred at rt. for further 2 h 40 min, before it was diluted with EtOAc (150 mL). The organic layer was washed three times with aq. 10% citric acid (3x150 mL), twice with aq. sat. $NaHCO_3$ (2x150 mL), once with brine (150 mL), dried over $MgSO_4$, filtered, and concentrated *in vacuo*. The residue (1.35 g) was purified by flash column chromatography on silica gel (hexane/EtOAc 7:3 + 1% Et_3N → 4:6 + 1% Et_3N). Product **4** was isolated as a yellow foam (490 mg, 0.64 mmol, 38%). R_f = 0.30 (hexane/EtOAc 4:6 + 1% Et_3N); ^{1}H NMR (400 MHz, CD_3CN) δ 7.49–7.45 (m, 2H), 7.36–7.32 (m, 4H), 7.30–7.19 (m, 3H), 7.16–7.11 (m, 10H), 7.04–7.00 (m, 4H), 6.98–6.94 (m, 4H), 6.86–6.82 (m, 4H), 3.75 (s, 6H), 3.63 (q, *J* = 6.3 Hz, 2H), 3.17 (t, *J* = 6.4 Hz, 2H), 2.92 (t, *J* = 5.3 Hz, 1H), 2.60 (t, *J* = 6.4 Hz, 2H), 2.53 (t, *J* = 6.6 Hz, 2H); ^{13}C NMR (101 MHz, CD_3CN) δ 159.66, 146.26, 144.30, 144.08, 142.01, 141.99, 137.19, 132.07, 132.02, 131.96, 131.72, 131.68, 130.93, 128.99, 128.87, 128.81, 127.82, 127.80, 122.82, 114.02, 89.58, 62.84, 61.35, 55.90, 24.27, 21.43; HRMS-NSI (*m/z*): $[M]^+$ calcd for $C_{55}H_{46}O_4$, 770.3391; found, 770.3401.

(*E*)-4-(4-(2-(4-(4-(bis(4-methoxyphenyl)(phenyl)methoxy)but-1-yn-1-yl)phenyl)-1,2diphenylvinyl)phenyl) but-3-yn-1-yl (2-cyanoethyl) diisopropylphosphoramidite (5)

Starting material **4** (460 mg, 0.60 mmol) was dissolved in DCM (6 mL) and Hünig's base (0.3 mL). CEP-Cl (143 mg, 0.60 mmol) was added dropwise to the clear, yellow solution at rt. The RM was stirred at rt. for 2 h. The

yellowish RM was concentrated *in vacuo*. The crude product (760 mg) was purified by a short flash column chromatography on silica gel (hexane/EtOAc 7:3 + 1% Et_3N). Product **5** was isolated as a yellowish foam (509 mg, 0.52 mmol, 87%). R_f = 0.55 (hexane/EtOAc 6:4 + 1% Et_3N); ^{1}H NMR (400 MHz, DMSO-d_6) δ 7.45–7.41 (m, 2H), 7.30–7.11 (m, 17H), 6.99–6.84 (m, 12H), 3.80–3.65 (m, 10H), 3.62–3.52 (m, 2H), 3.10 (t, *J* = 6.4 Hz, 2H), 2.75 (td, *J* = 6.4, 1.4 Hz, 2H), 2.66 (q, *J* = 6.2 Hz, 4H), 1.12 (dd, *J* = 6.5, 5.7 Hz, 12H); ^{13}C NMR (101 MHz, DMSO-d_6) δ 158.05, 144.83, 142.73, 142.70, 142.52, 142.50, 140.45, 140.44, 135.63, 130.83, 130.76, 130.66, 130.62, 129.59, 127.96, 127.79, 127.61, 126.84, 126.82, 126.64, 121.14, 121.11, 118.90, 113.15, 88.73, 88.17, 85.44, 81.18, 81.13, 61.59, 61.47, 61.29, 58.34, 58.16, 54.99, 42.58, 42.45, 24.36, 24.35, 24.29, 24.28, 21.77, 21.70, 20.18, 19.81, 19.74; ^{31}P NMR (162 MHz, DMSO-d_6) δ 147.13; HRMS-NSI (*m/z*): $[M+H]^+$ calcd for $C_{64}H_{64}O_5N_2P$, 971.4558; found, 971.4565.

***E*-TPE-modified solid-support (7)**

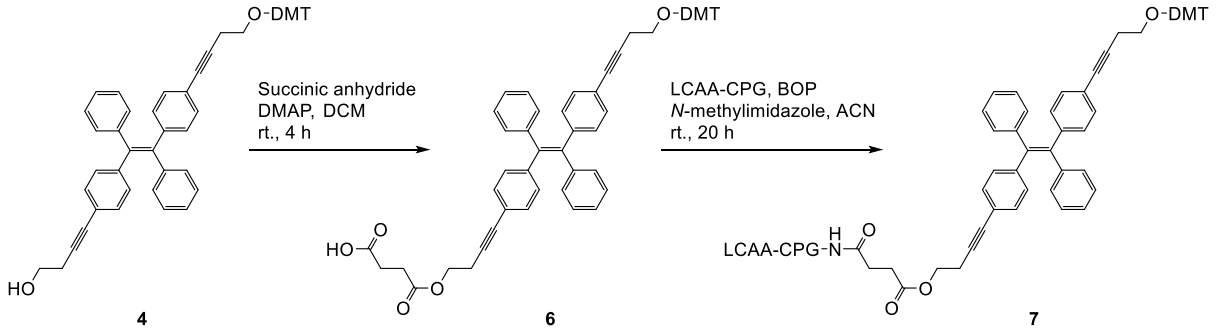

Scheme S2: Synthetic approach for *E*-TPE-modified solid-support **7**.

The synthesis of *E*-TPE-modified solid-support **7** was adapted from published procedures.[4] Compound **4** (31.2 mg, 0.04 mmol) was dissolved in DCM (0.2 mL). Succinic anhydride (4.1 mg, 0.04 mmol), followed by DMAP (7.9 mg, 0.06 mmol) were added and the RM was stirred at rt. for 4 h. The RM was diluted with DCM (3 mL) and the organic layer was washed once with aq. 10% citric acid (5 mL), once with brine (5 mL), dried over $MgSO_4$, filtered, and concentrated *in vacuo* to yield compound **6**. Compound **6** was dissolved in acetonitrile (3 mL) and 2.8 mL of this solution (about 37 μmol of compound **6**) was added to LCAA-CPG (301.3 mg, 500 Å, amine loading: 82 μmol/g). BOP (33.8 mg, 0.08 mmol) and *N*-methylimidazole (12 μL, 0.15 mmol) were added. The suspension was shaken at rt. for 20 h. The solid-support **7** was filtered off and washed with acetonitrile and DCM. A solution of pyridine and acetic anhydride (3:1, 3.6 mL) was added to the solid-support **7**. DMAP (32.3 mg, 0.26 mmol) was added and the suspension was shaken at rt. for 2 h. The solid-support **7** was filtered off and washed with DCM. The loading was determined according to the Beer-Lambert law: solid-support **7** (2.5 mg) was added to 3% trichloroacetic acid in DCM (10 mL). After a 1:1 dilution, the absorbance was measured at 498 nm. For the calculation of the loading, a molar absorptivity of the DMT cation of ε: 70'000 L/mol·cm was used. The loading of solid-support **7** was calculated to be 70 μmol/g.

4. NMR spectra

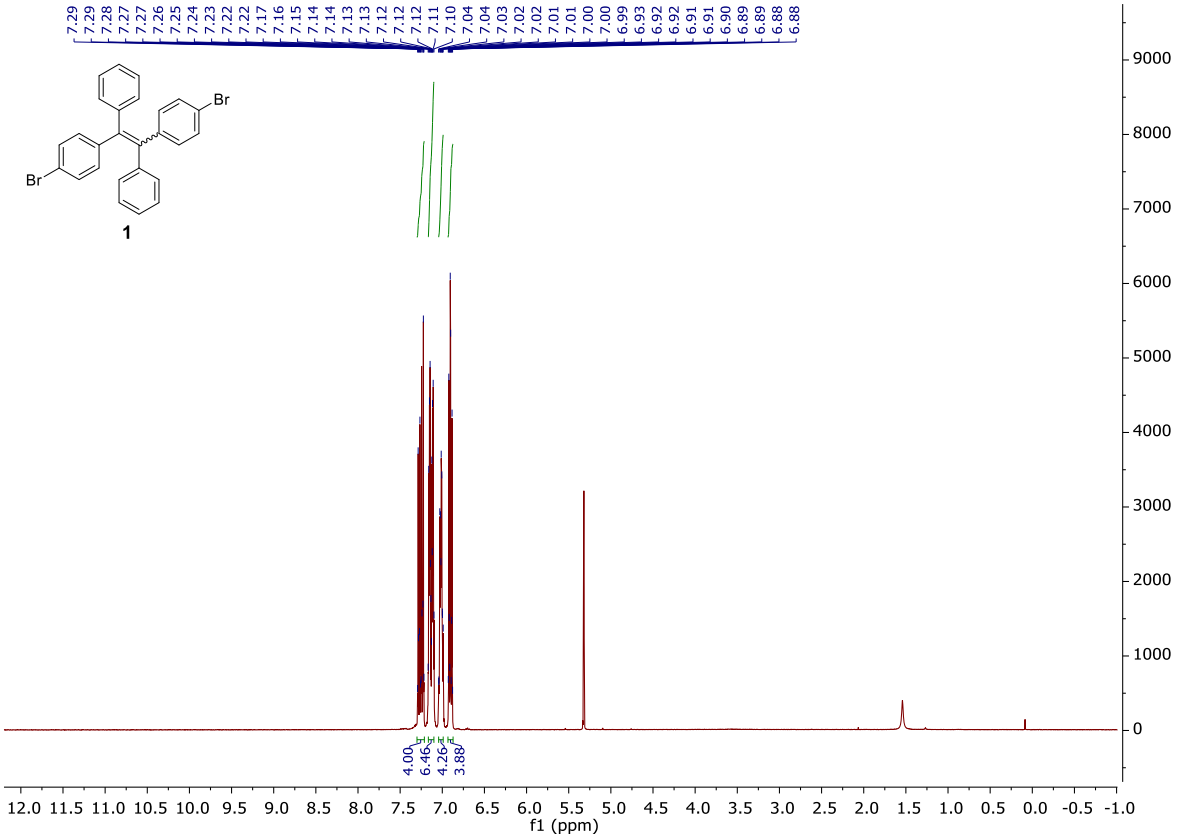

Fig. S1: ^{1}H NMR of compound **1** in DCM-d_2.

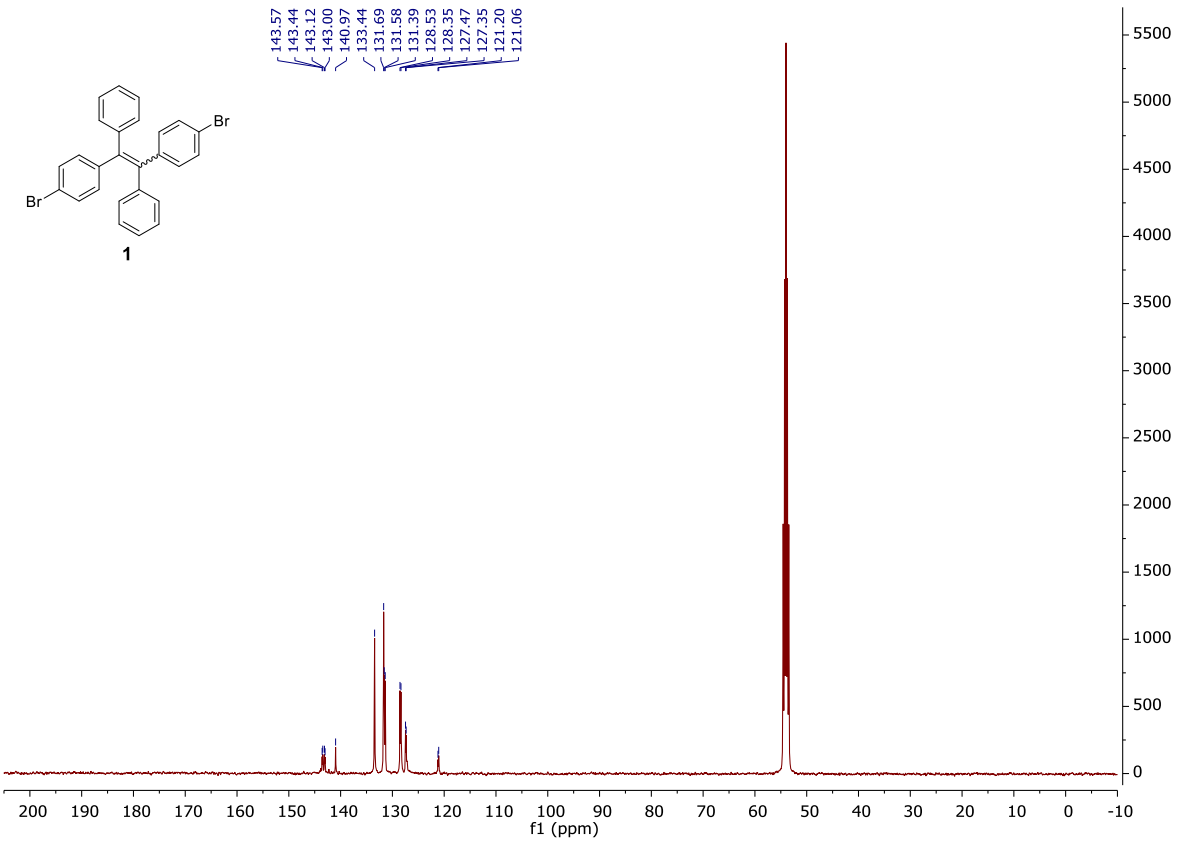

Fig. S2: ^{13}C NMR of compound **1** in DCM-d_2.

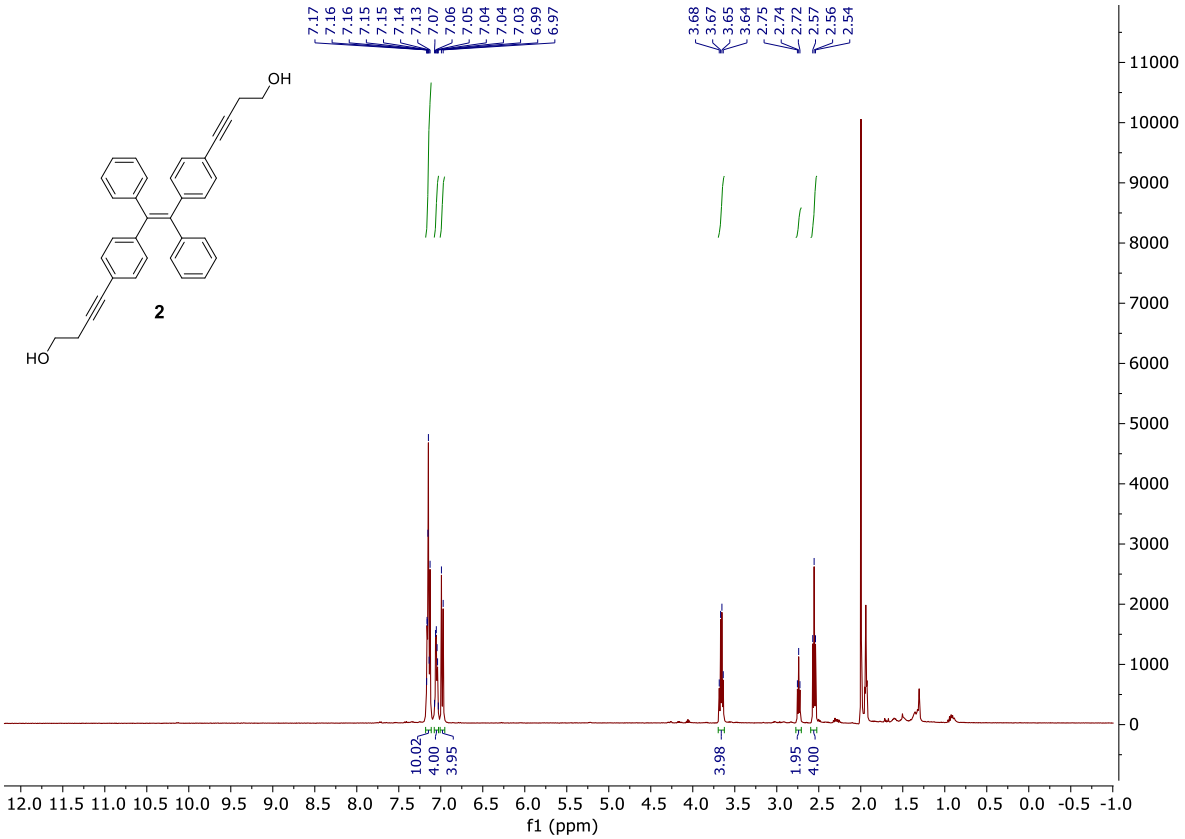

Fig. S3: ^{1}H NMR of compound **2** in CD_3CN at 333 K.

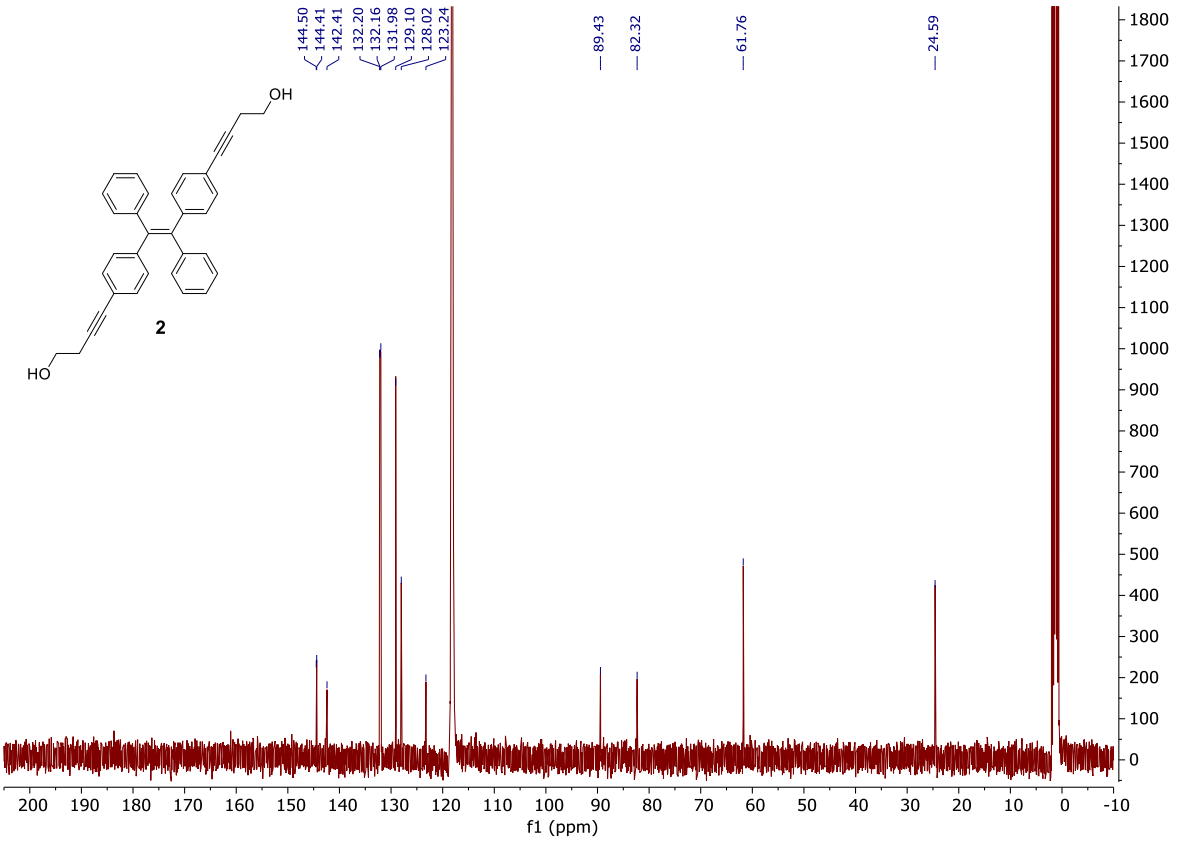

Fig. S4: ^{13}C NMR of compound **2** in CD_3CN at 333 K.

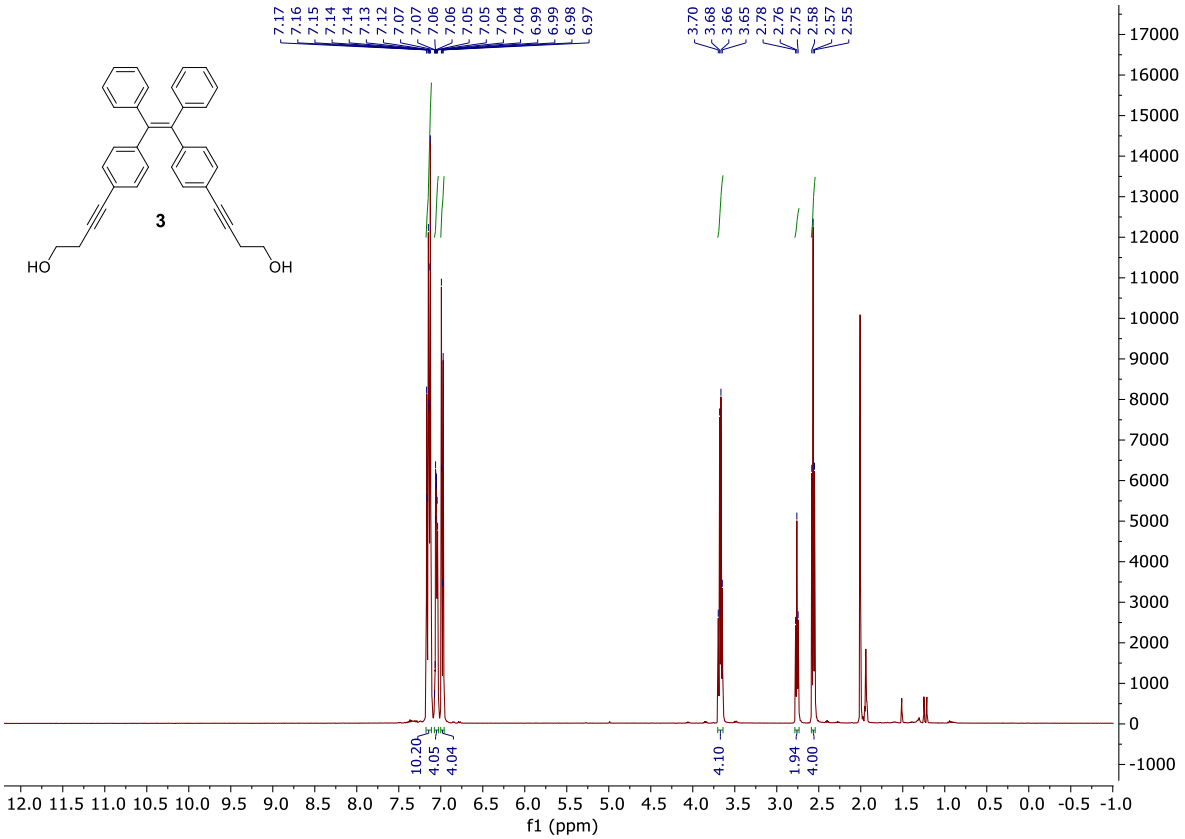

Fig. S5: ^{1}H NMR of compound **3** in CD_3CN at 333 K.

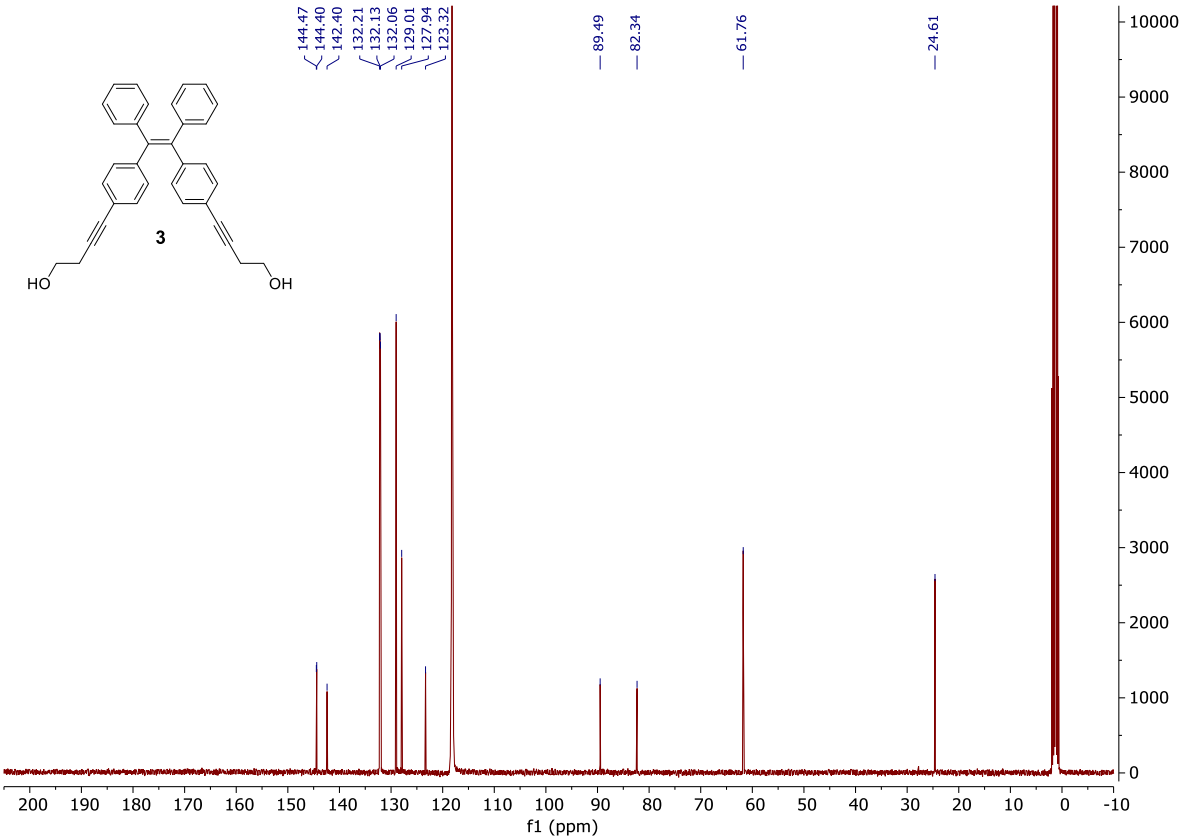

Fig. S6: ^{13}C NMR of compound **3** in CD_3CN at 333 K.

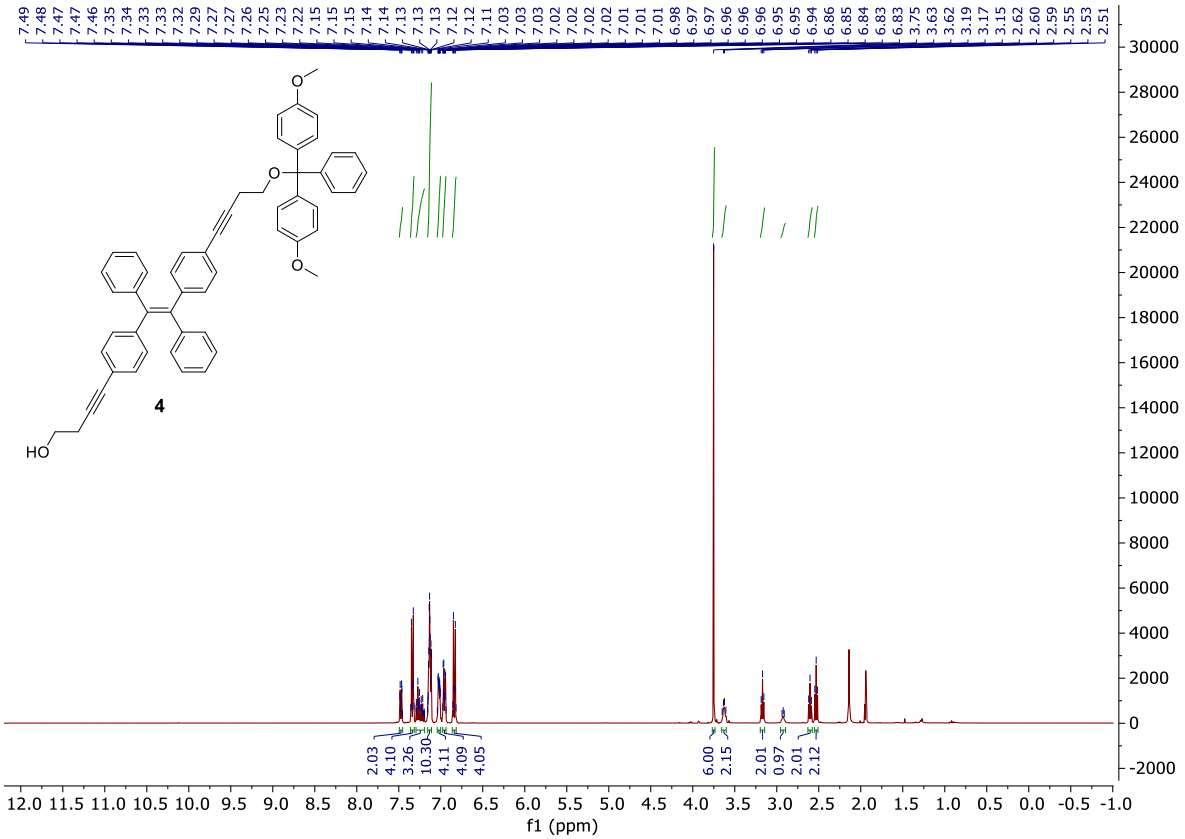

Fig. S7: ^{1}H NMR of compound **4** in CD_3CN.

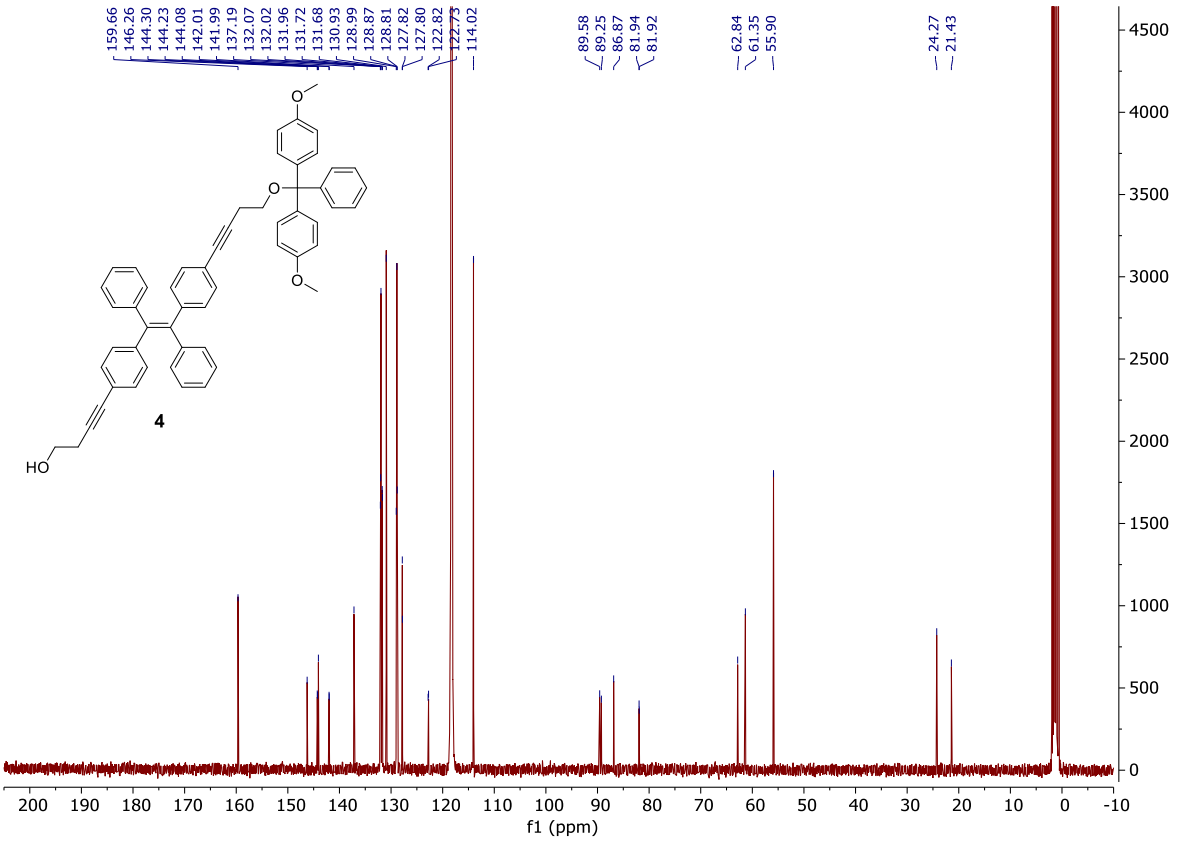

Fig. S8: ^{13}C NMR of compound **4** in CD_3CN.

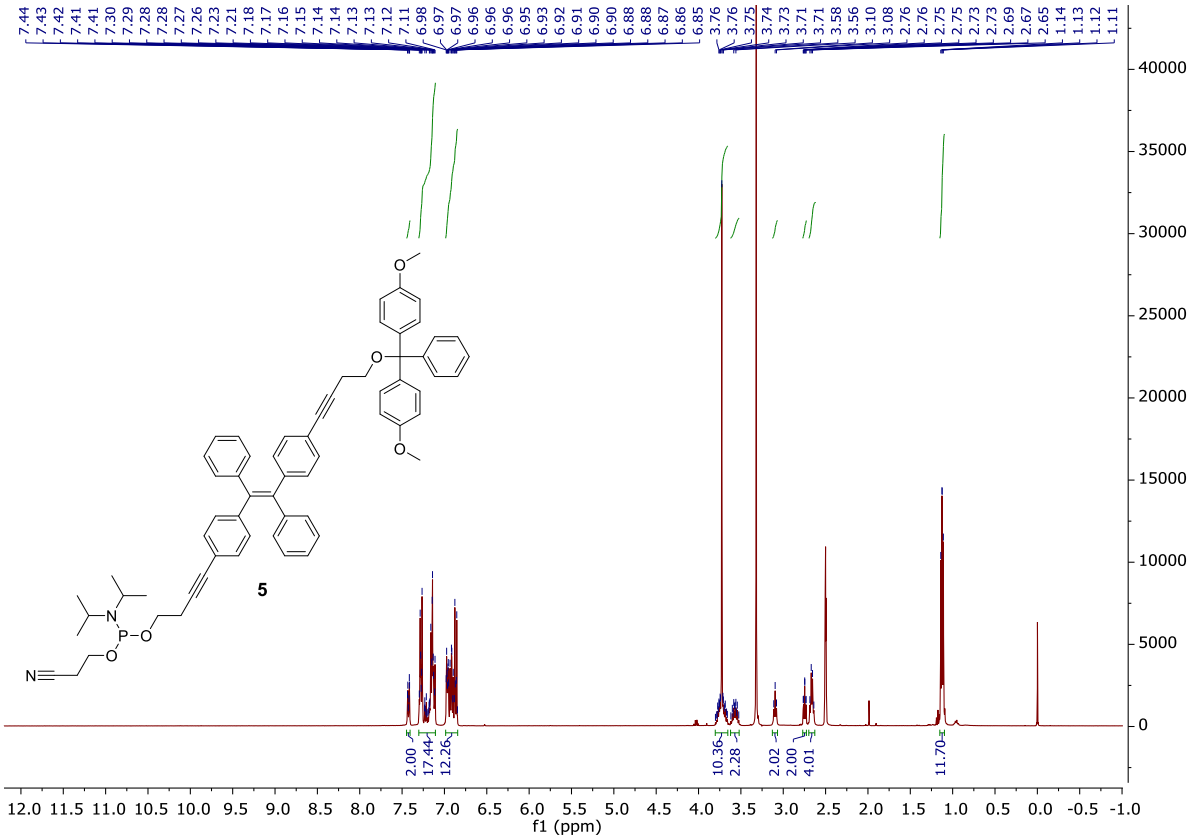

Fig. S9: ^{1}H NMR of compound **5** in DMSO-d_6.

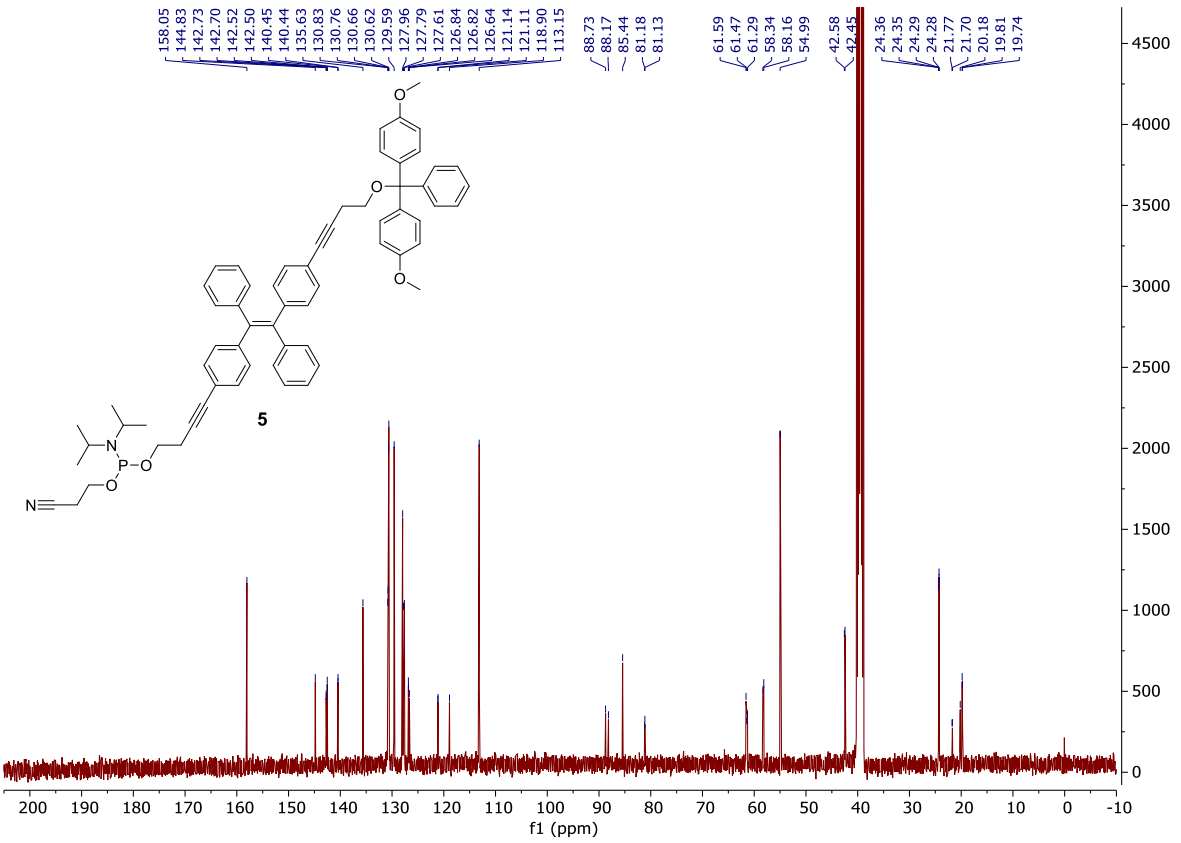

Fig. S10: ^{13}C NMR of compound **5** in DMSO-d_6.

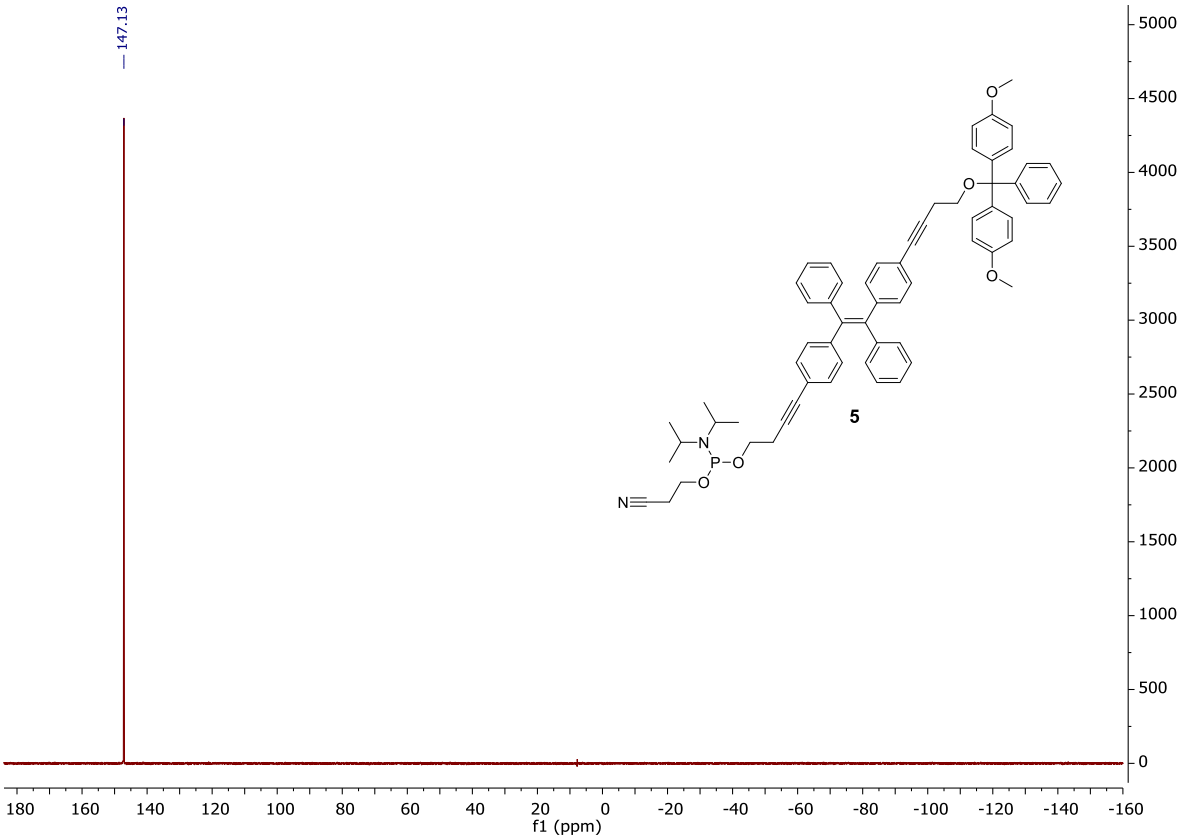

Fig. S11: ^{31}P NMR of compound **5** in DMSO-d_6.

5. Solid-phase oligomer synthesis

E-TPE-DNA conjugates **A** and **B** were synthesized on an Applied Biosystems 394 DNA/RNA synthesizer applying a standard cyanoethyl phosphoramidite coupling protocol on a 1 μmol scale. A coupling time of 30 s was employed for the DNA nucleobases and 2 min for the *E*-TPE modifications. *E*-TPE phosphoramidite **5** was dissolved in 1,2-dichloroethane to create a 0.1 M solution. The synthesis was started with *E*-TPE-modified solid-support **7**. After the solid-phase synthesis, the *E*-TPE-DNA conjugates **A** and **B** were cleaved and deprotected by treatment with aqueous NH_4OH (28-30%) at 55 °C overnight. The supernatants were collected, and the solid-support was washed three times with a solution of ethanol and Milli-Q H_2O (1:1, 3x1 mL), before the crude *E*-TPE-DNA conjugates **A** and **B** were lyophilized.

Oligomers **A** and **B** were purified by reversed-phase HPLC (*Shimadzu LC-20AT*, *LiChrospher 100 RP-18*, 5 μm) at 40 °C with a flow rate of 1 mL/min. Solvent A: 50 mM aqueous NH_4OAc; solvent B: acetonitrile; B [%] (t_R [min]) = 20 (0), 60 (24). The purified *E*-TPE-DNA conjugates **A** and **B** were dissolved in Milli-Q H_2O (1 mL). The absorbance was measured at 260 nm to determine the concentration of the stock solutions and was calculated according to the Beer-Lambert law. The following molar absorptivities (at 260 nm) in [L/mol·cm] were used for the DNA nucleobases: ε_A: 15'300; ε_T: 9'000; ε_G: 11'700; ε_C: 7'400. A molar absorptivity of $\varepsilon_{E\text{-TPE}}$: 35'975 was used for *E*-TPE. *E*-TPE-DNA conjugate **A** was obtained in 34% yield; oligomer **B** in 36% yield. The corresponding HPLC traces of **A** and **B** are displayed in Fig. S12.

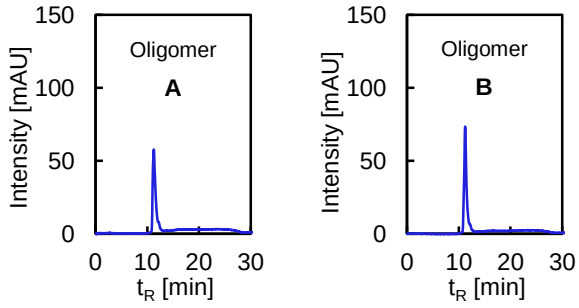

Fig. S12: HPLC traces for **A** and **B**.

Table S1: Calculated and found masses of **A** and **B** by ESI-MS (negative ion mode).

Oligomer	calcd.	found
A	7790.6101	555.4642 (z=14)
B	7625.4699	761.5454 (z=10)

6. Sequences of DNA single strands

Oligomers **C** and **D** served as control and reference strands. Cy3-labelled oligomer **E** is complementary to strand **A**, whereas strand **F** is non-complementary to either TPE-DNA conjugate **A** or **B** and was used as control.

Table S2: Summary of all DNA single strands that were utilized in this study.

Strand	Sequence
A	5'-CAA GGT CCG ATG CAA GGA AG-(***E*-TPE**)$_3$
B	(***E*-TPE**)$_3$-GTT CCA GGC TAC GTT CCT TC-5'
C	5'-CAA GGT CCG ATG CAA GGA AG-3'
D	3'-GTT CCA GGC TAC GTT CCT TC-5'
E	3'-GTT CCA GGC TAC GTT CCT TC-(**Cy3**)
F	3'-TCG TTC TAG CCT AGC TTC CG-(**Cy3**)

7. UV-vis and fluorescence spectra of *E*-TPE diol (2)

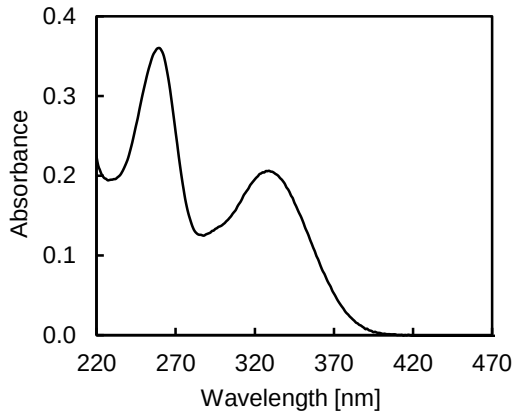

Fig. S13: Absorption spectrum of *E*-TPE diol **2** at a concentration of 10 μM in ethanol at 20 °C.

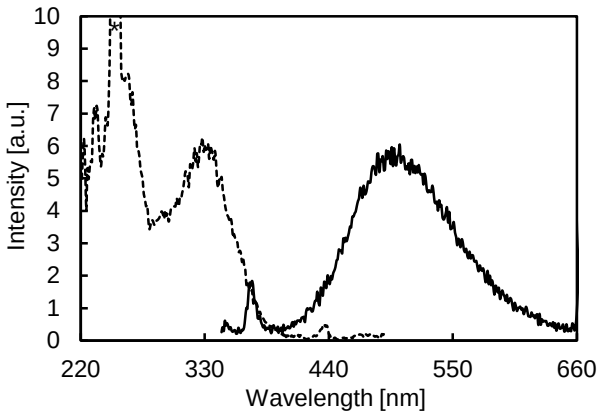

Fig. S14: Excitation (dotted line) and emission (solid line) spectra of *E*-TPE diol **2**. Conditions: 10 μM of **2** in ethanol, $\lambda_{ex.}$: 335 nm, $\lambda_{em.}$: 500 nm, excitation slit: 5 nm, emission slit: 5 nm, 20 °C, * indicates a second order diffraction.

8. Cryo-EM images

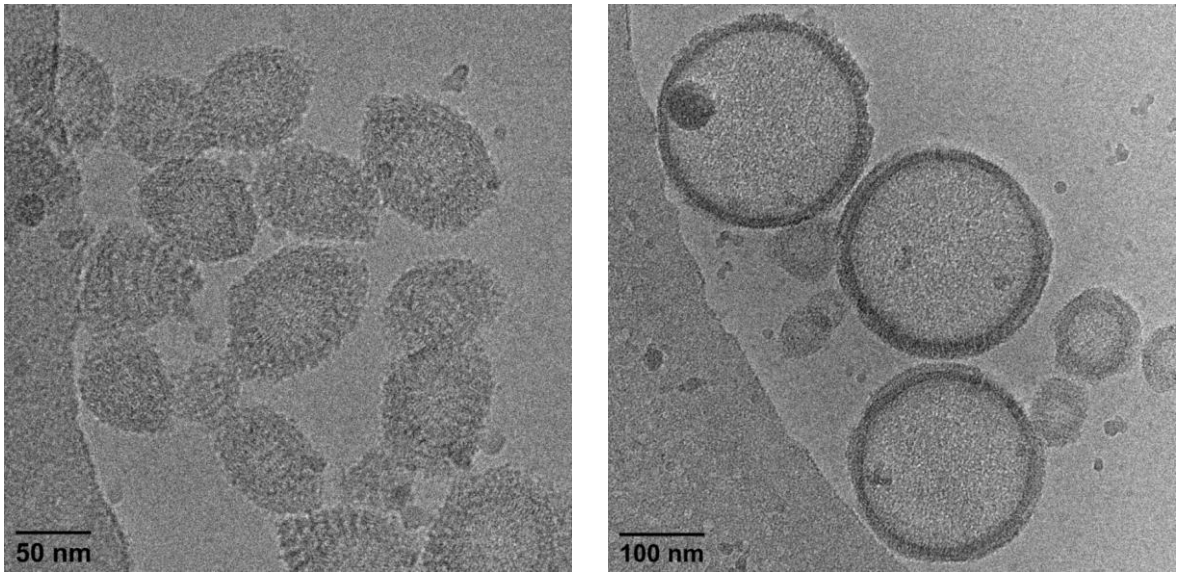

Fig. S15: Enlarged cryo-EM images from the main text of type I and II vesicles. Conditions: 1 μM **A*B**, 10 mM sodium phosphate buffer pH 7.2, 0.1 mM spermine · 4 HCl, 20 vol% ethanol.

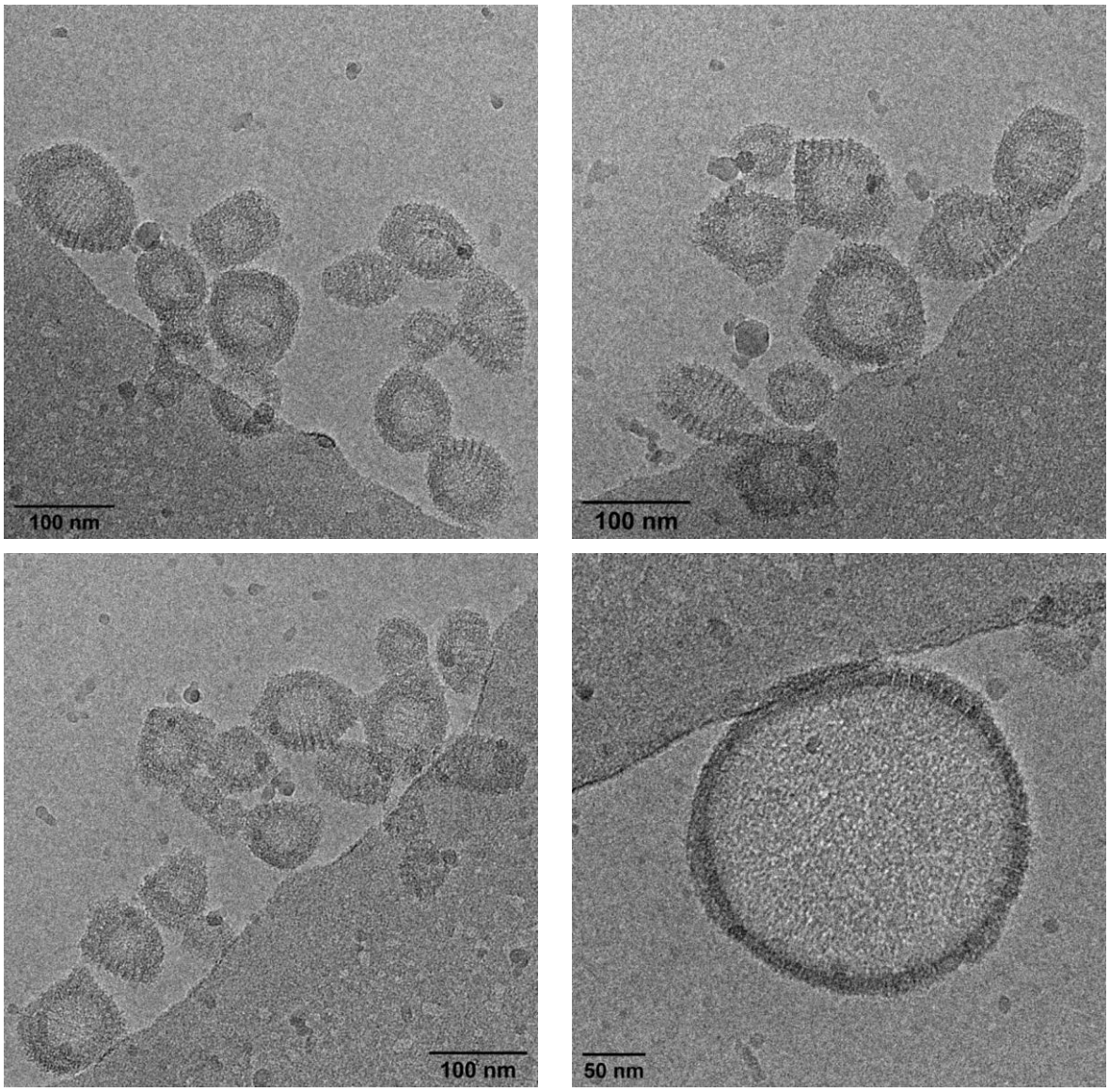

Fig. S16: Additional cryo-EM images of type I and II vesicles. Conditions: 1 μM **A*B**, 10 mM sodium phosphate buffer pH 7.2, 0.1 mM spermine · 4 HCl, 20 vol% ethanol.

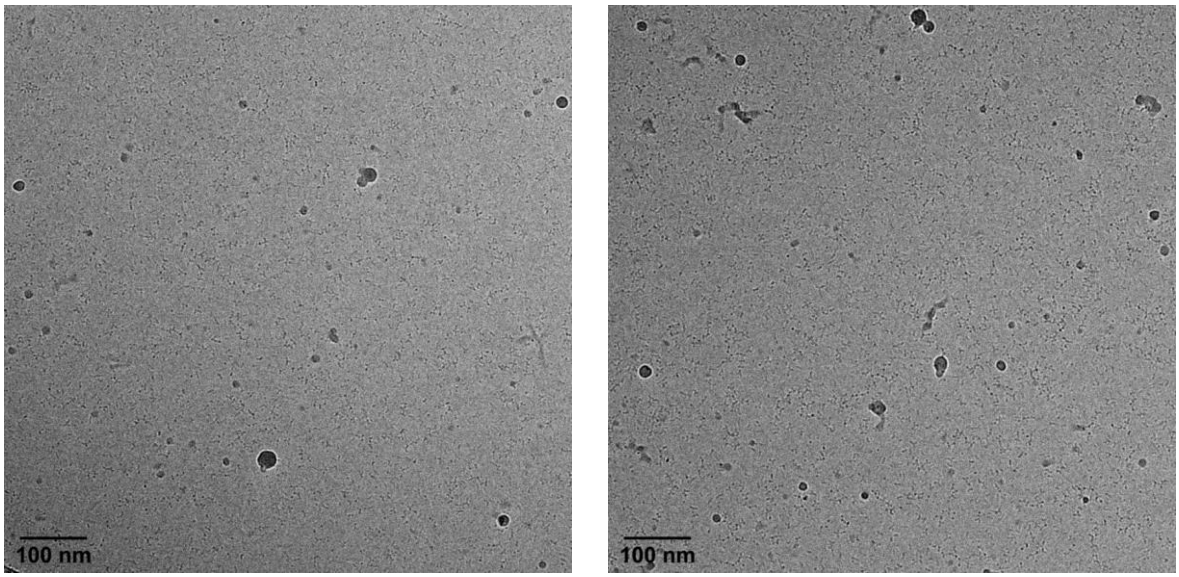

Fig. S17: Cryo-EM images of **A*B** in the absence of spermine · 4 HCl. Conditions: 1 μM **A*B**, 10 mM sodium phosphate buffer pH 7.2, 20 vol% ethanol.

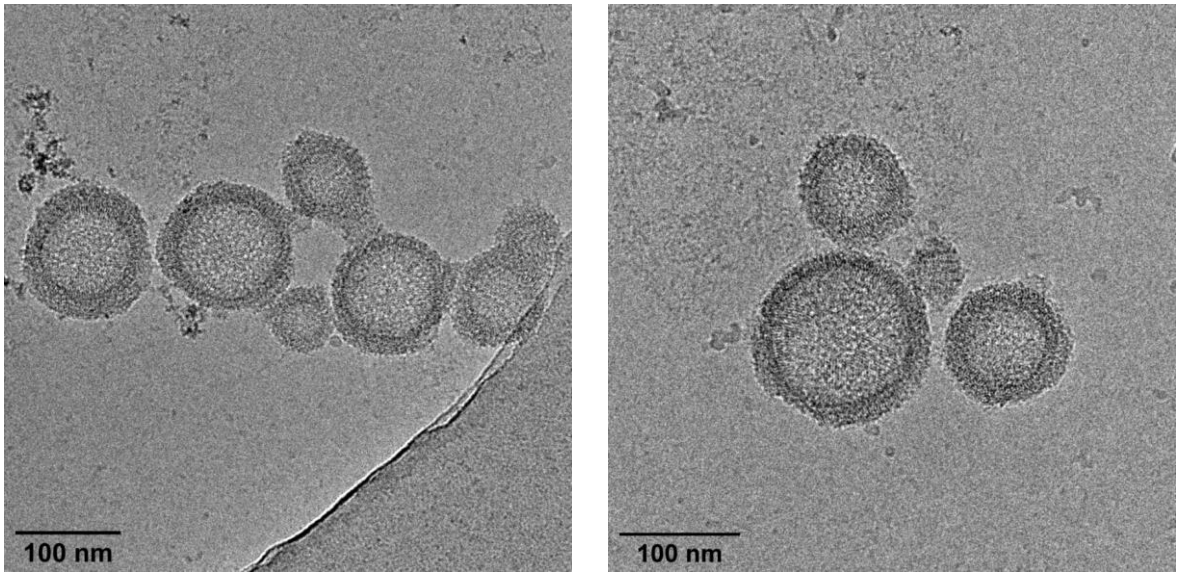

Fig. S18: Enlarged cryo-EM images from the main text of vesicles after dialysis. Conditions: 1 μM **A*B**, 10 mM sodium phosphate buffer pH 7.2, 0.1 mM spermine · 4 HCl, < 0.5 vol% ethanol.

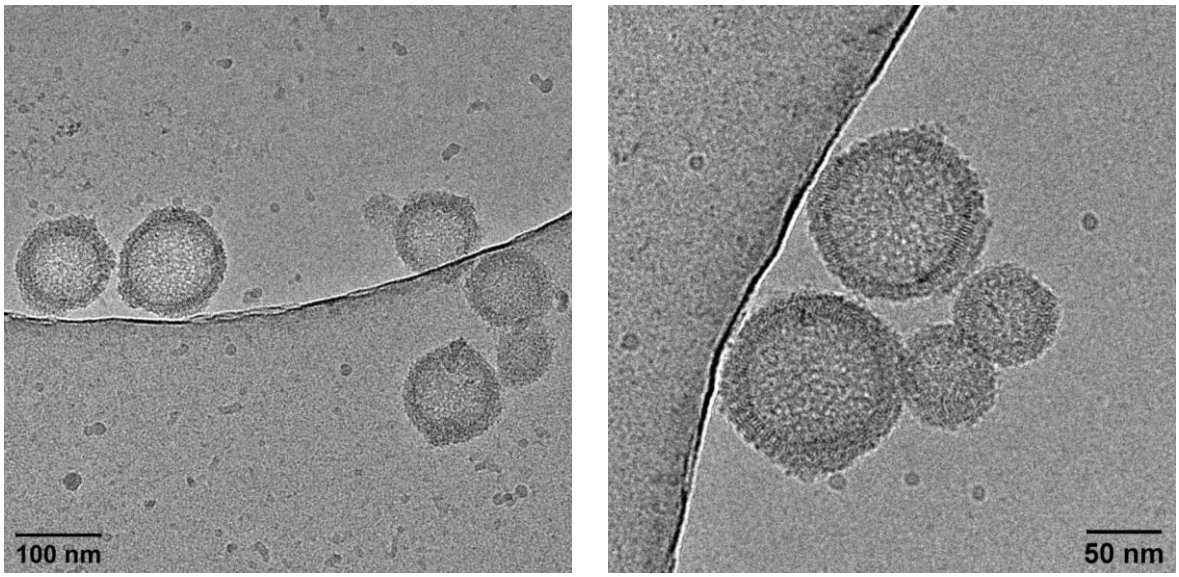

Fig. S19: Additional cryo-EM images of vesicles after dialysis. Conditions: 1 μM **A*B**, 10 mM sodium phosphate buffer pH 7.2, 0.1 mM spermine · 4 HCl, < 0.5 vol% ethanol.

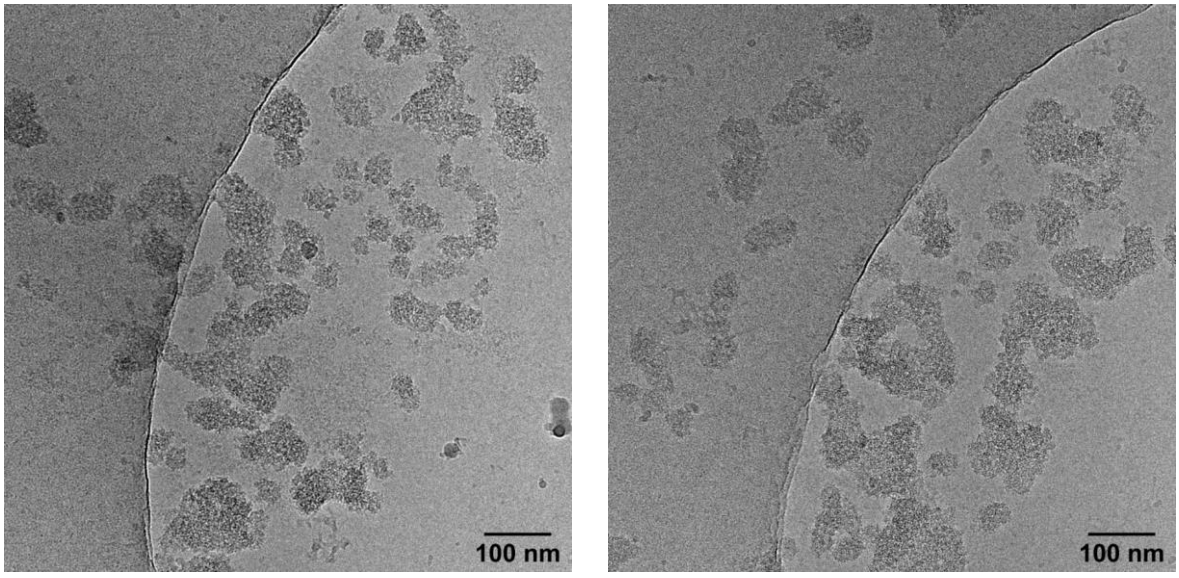

Fig. S20: Cryo-EM images of aggregates that were prepared in the absence of the ethanol fraction. Conditions: 1 μM **A*B**, 10 mM sodium phosphate buffer pH 7.2, 0.1 mM spermine · 4 HCl.

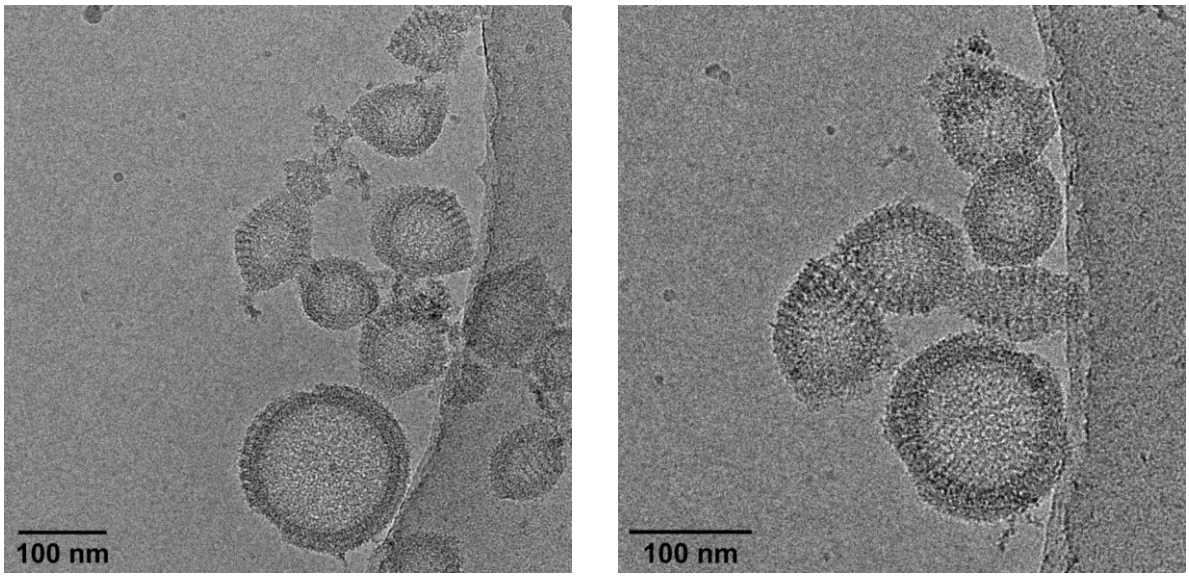

Fig. S21: Cryo-EM images of vesicles after EthBr addition. Conditions: 1 μM **A*B**, 10 μM EthBr, 10 mM sodium phosphate buffer pH 7.2, 0.1 mM spermine · 4 HCl, 20 vol% ethanol.

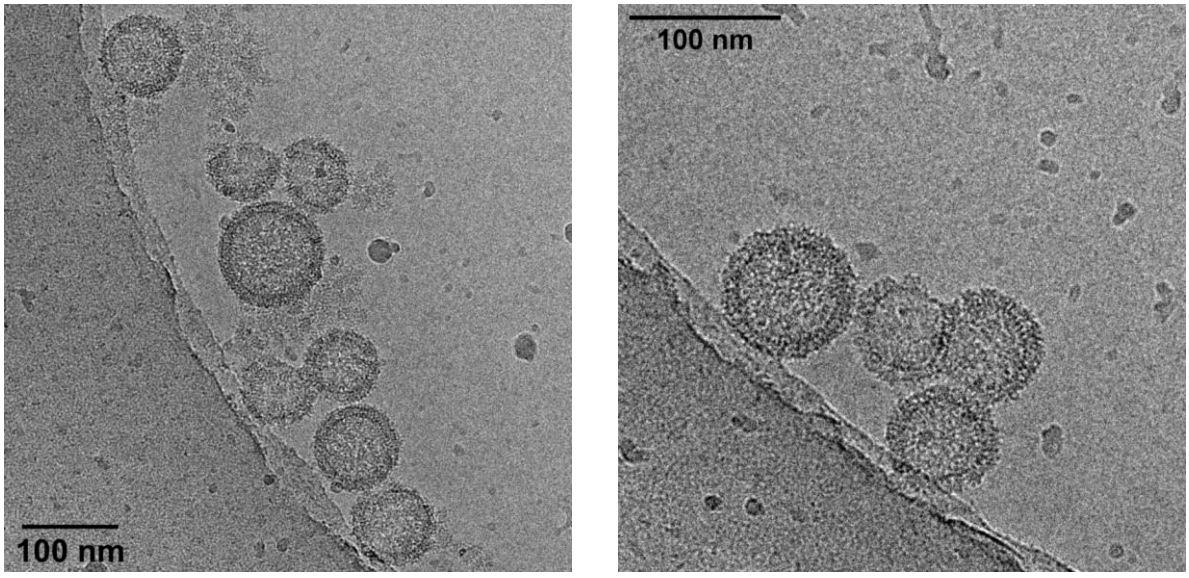

Fig. S22: Cryo-EM images of vesicles after dialysis and after EthBr addition. Conditions: 1 μM **A*B**, 10 μM EthBr, 10 mM sodium phosphate buffer pH 7.2, 0.1 mM spermine · 4 HCl, < 0.5 vol% ethanol.

9. AFM images

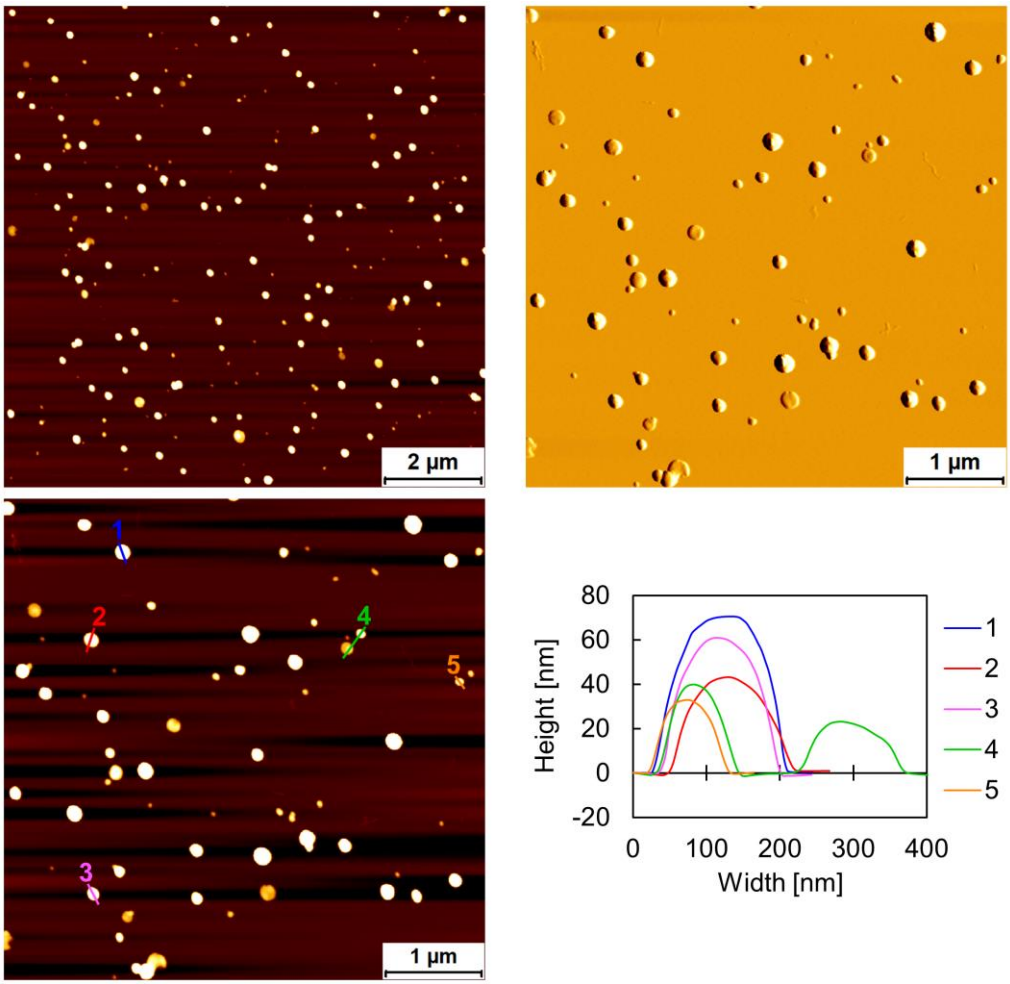

Fig. S23: AFM overview scan (top left), deflection scan (top right), and zoom with corresponding cross sections (bottom) of assembled TPE-DNA conjugates **A*B**. Conditions: 1 µM **A*B**, 10 mM sodium phosphate buffer pH 7.2, 0.1 mM spermine · 4 HCl, 20 vol% ethanol.

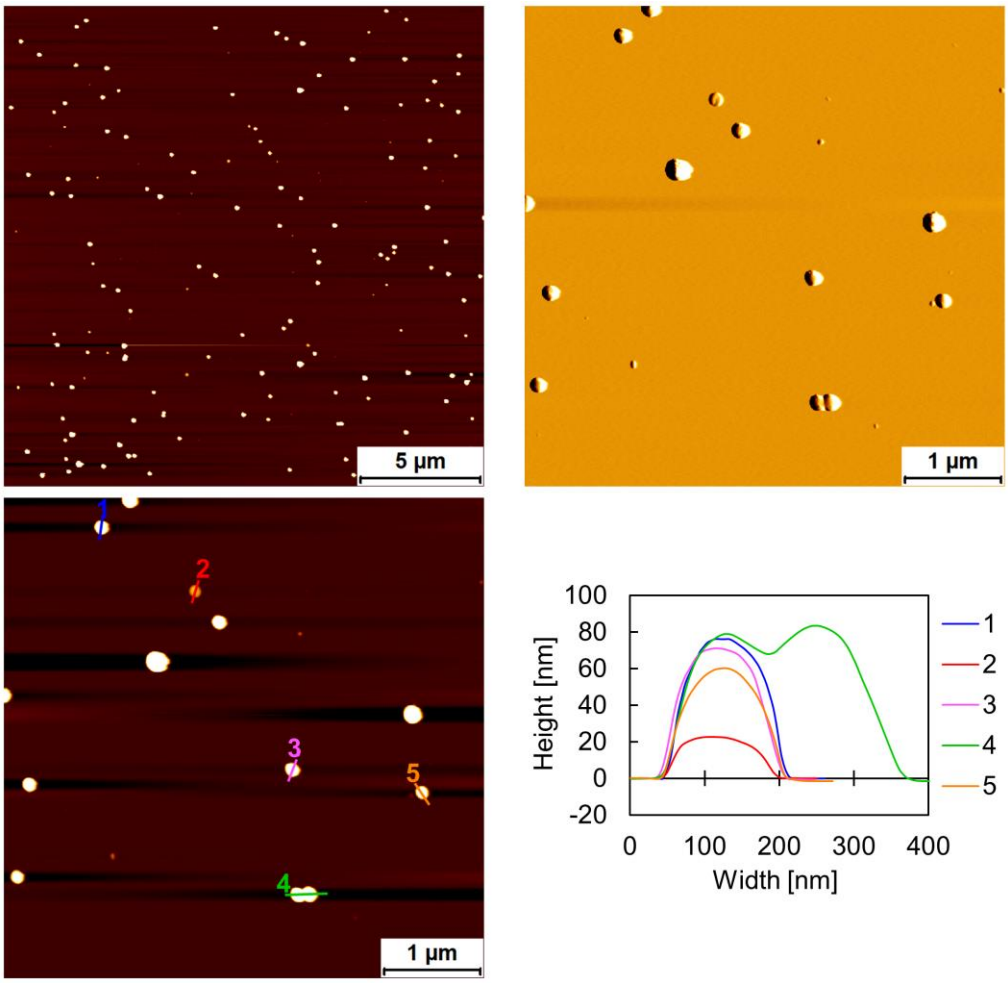

Fig. S24: AFM overview scan (top left), deflection scan (top right), and zoom with corresponding cross sections (bottom) of Cy3 doped assemblies of **A*B**. Conditions: 1 µM **A*B**, 1 mol% **E**, 10 mM sodium phosphate buffer pH 7.2, 0.1 mM spermine · 4 HCl, 20 vol% ethanol.

10. Refractive index calibration curve

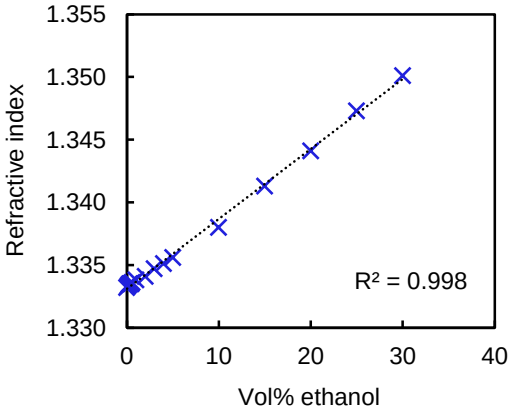

Vol% ethanol	n_D^{20}	Vol% ethanol	n_D^{20}
0	1.3332	3	1.3347
0.1	1.3333	4	1.3351
0.2	1.3334	5	1.3356
0.3	1.3335	10	1.3380
0.4	1.3335	15	1.3413
0.5	1.3335	20	1.3441
0.6	1.3336	25	1.3473
1	1.3338	30	1.3501
2	1.3341		

Fig. S25: Refractive index (n_D^{20}) calibration curve of aqueous medium. Conditions: 10 mM sodium phosphate buffer pH 7.2, 0.1 mM spermine · 4 HCl, varying ethanol fraction.

11. UV-vis absorption spectrum of A*B

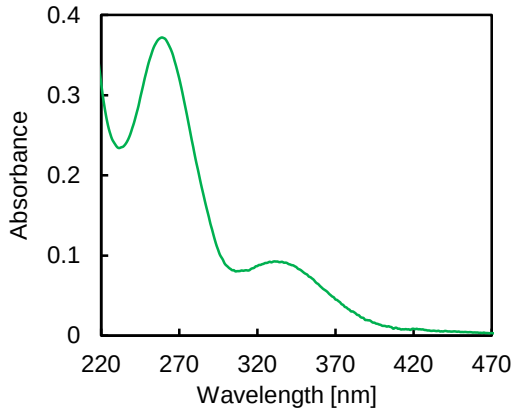

Fig. S26: UV-vis absorption spectrum of **A*B** after dialysis. Conditions: 1 μM **A*B**, 10 mM sodium phosphate buffer pH 7.2, 0.1 mM spermine · 4 HCl, < 0.5 vol% ethanol, 20 °C.

12. UV-vis monitored denaturation curves of A*B

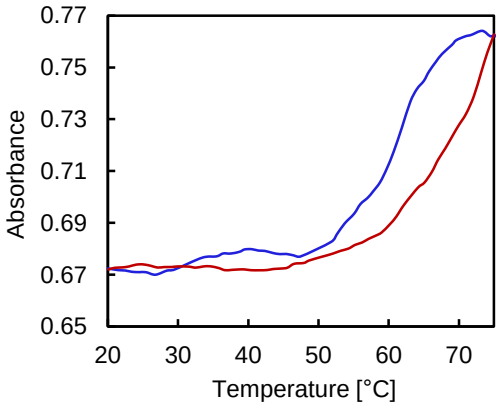

Fig. S27: UV-vis monitored annealing (blue) and melting (red) curves of **A*B**. Conditions: 1 μM **A*B**, 10 mM sodium phosphate buffer pH 7.2, 0.1 mM spermine · 4 HCl, 20 vol% ethanol, λ_{abs}: 260 nm, temperature gradient: 0.5 °C/min.

13. Fluorescence quantum yield (Φ_{FL}) determination

Fluorescence quantum yields (Φ_{FL}) of 1 µM **A*B** in aqueous medium (10 mM sodium phosphate buffer pH 7.2, 0.1 mM spermine · 4 HCl, 20 resp. < 0.5 vol% ethanol) were determined according to published procedures[6] relative to quinine sulfate (in 0.5 M sulfuric acid) as a standard.[7]

Table S3: Mean values for the calculation of fluorescence quantum yields. [a] Absorbance at the excitation wavelength of 335 nm. [b] Integrated fluorescence intensity between 360–660 nm, $\lambda_{ex.}$: 335 nm. [c] Refractive index of the medium at 20.00 °C.

	$Abs_{335\ nm}$ [a]	FL_{area} [b]	n_D^{20} [c]	Φ_{FL} [%]
75 °C, disassembled **A**, **B**	0.1293	193.9	1.3441	< 0.75
20 °C, **A*B** after assembly process	0.1344	17494.5	1.3441	31 ± 1
20 °C, **A*B** after dialysis	0.0961	9386.2	1.3332	23 ± 2

14. Ethidium bromide experiments

Fig. S28: Visualization of maximally EthBr (red) intercalated 20-mer DNA duplex **C*D** considering the neighbor exclusion principle.[8]

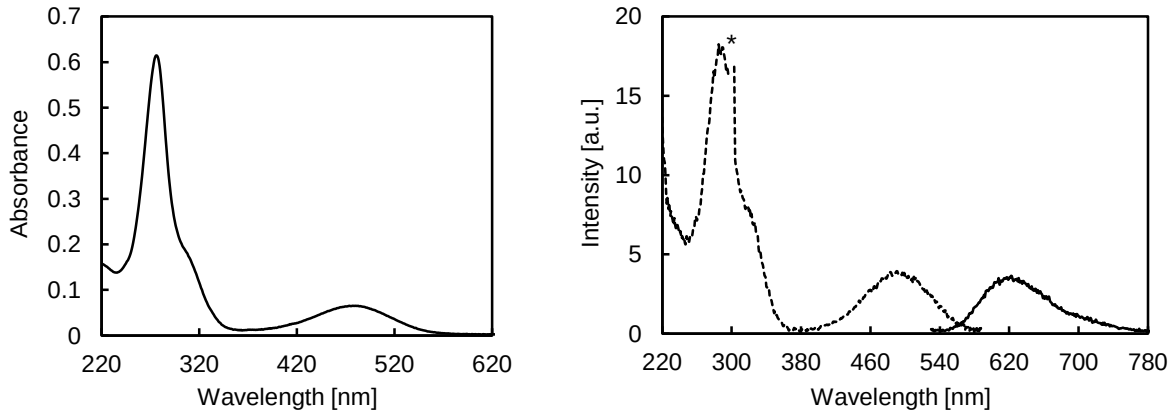

Fig. S29: Absorption spectrum (left), fluorescence emission spectrum (right, solid line), and excitation spectrum (right, dotted line) of EthBr in aqueous medium containing 20 vol% ethanol. Conditions: 10 µM EthBr, 10 mM sodium phosphate buffer pH 7.2, 0.1 mM spermine · 4 HCl, 20 vol% ethanol, $\lambda_{ex.}$: 520 nm, $\lambda_{em.}$: 600 nm, 20 °C, * indicates a second order diffraction.

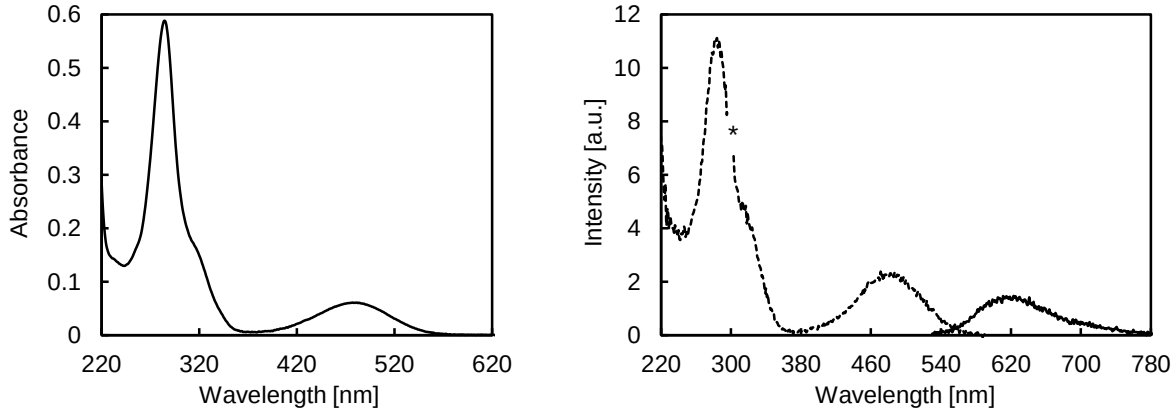

Fig. S30: Absorption spectrum (left), fluorescence emission spectrum (right, solid line), and excitation spectrum (right, dotted line) of EthBr in aqueous medium. Conditions: 10 µM EthBr, 10 mM sodium phosphate buffer pH 7.2, 0.1 mM spermine · 4 HCl, $\lambda_{ex.}$: 520 nm, $\lambda_{em.}$: 600 nm, 20 °C, * indicates a second order diffraction.

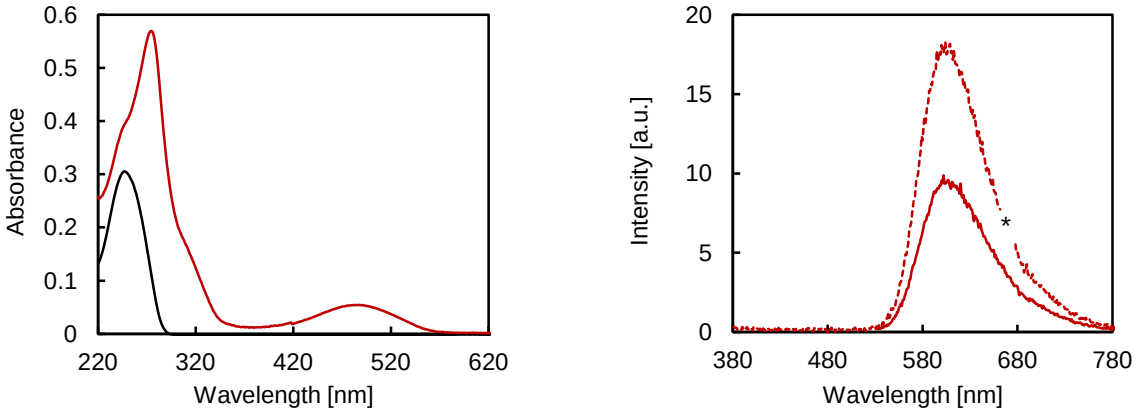

Fig. S31: Absorption spectra (left) and fluorescence emission spectra (right) of **C*D** (1 µM) in aqueous medium (10 mM sodium phosphate buffer pH 7.2, 0.1 mM spermine · 4 HCl, 20 vol% ethanol) after thermally controlled assembly process at 20 °C (black), and after the addition of 10 µM EthBr at 20 °C (red). Solid line: $\lambda_{ex.}$: 520 nm, dotted line: $\lambda_{ex.}$: 335 nm, * indicates a second order diffraction.

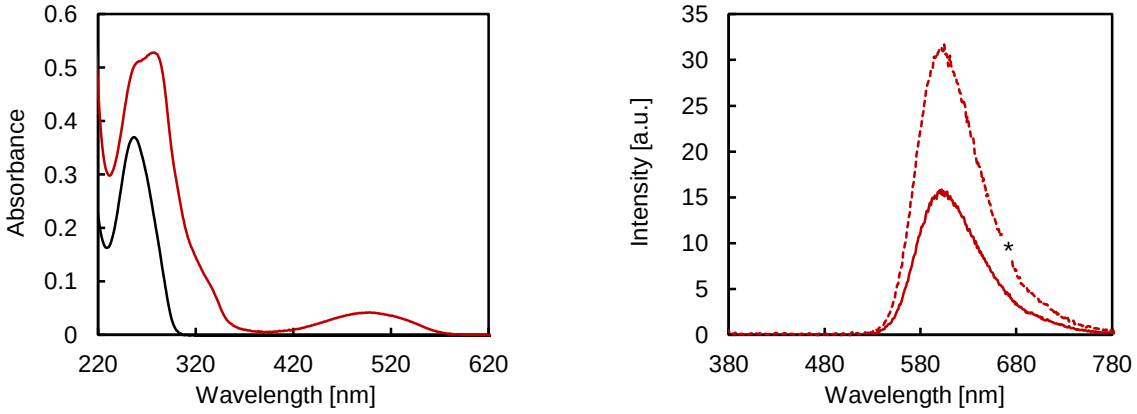

Fig. S32: Absorption spectra (left) and fluorescence emission spectra (right) of **C*D** (1 µM) in aqueous medium (10 mM sodium phosphate buffer pH 7.2, 0.1 mM spermine · 4 HCl) after thermally controlled assembly process at 20 °C (black), and after the addition of 10 µM EthBr at 20 °C (red). Solid line: $\lambda_{ex.}$: 520 nm, dotted line: $\lambda_{ex.}$: 335 nm, * indicates a second order diffraction.

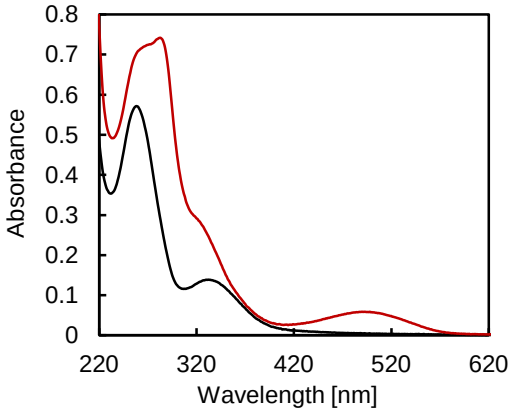

Fig. S33: Absorption spectra of assembled **A*B** in aqueous medium in the absence (black) and presence of 10 µM EthBr (red). Conditions: 1 µM **A*B**, 10 mM sodium phosphate buffer pH 7.2, 0.1 mM spermine · 4 HCl, 20 vol% ethanol, 20 °C.

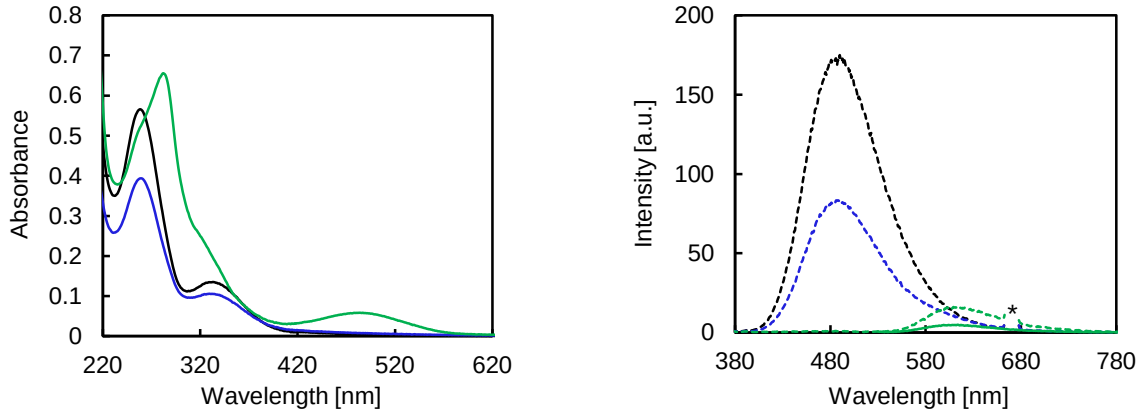

Fig. S34: Absorption spectra (left) and fluorescence emission spectra (right) of assembled **A*B** in aqueous medium at 20 °C in the absence of EthBr before (black) and after (blue) dialysis, and after dialysis in the presence of 10 µM EthBr (green). Conditions: 1 µM **A*B**, 10 mM sodium phosphate buffer pH 7.2, 0.1 mM spermine · 4 HCl, 20 resp. < 0.5 vol% ethanol, solid line: $\lambda_{ex.}$: 520 nm, dotted line: $\lambda_{ex.}$: 335 nm, * indicates a second order diffraction.

Table S4: Mean values for the calculation of the intercalation efficiency. Conditions: 1 µM each strand, 10 µM EthBr, 10 mM sodium phosphate buffer pH 7.2, 0.1 mM spermine · 4 HCl, 20 resp. < 0.5 vol% ethanol, 20 °C. [a] Integrated fluorescence intensity between 540–740 nm, $\lambda_{ex.}$: 520 nm. [b] Assuming that the unmodified DNA duplex **C*D** is fully loaded with a maximum of 10 EthBr moieties.

Sample	FL_{area} [a]	Sample-Blank	[%]	Number of intercalated EthBr
Aqueous medium, containing 20 vol% ethanol	362.8	0	0	0
C*D, containing 20 vol% ethanol	877.2	514.4	100[b]	10[b]
EthBr added to type I vesicles	655.2	292.4	57	6
Aqueous medium, without ethanol	149.9	0	0	0
C*D, without ethanol	1340.4	1190.5	100[b]	10[b]
EthBr added to type II architecture	434.1	284.2	24	2

15. Light-harvesting experiments

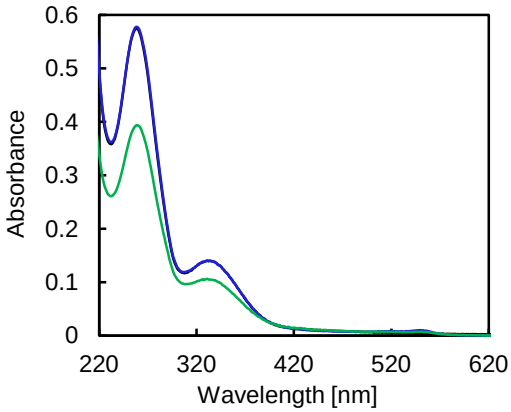

Fig. S35: UV-vis spectra of **A*B** in aqueous medium at 20 °C in the absence (black) and presence of 1 mol% **E** before (blue) and after (green) dialysis. Conditions: 1 μM **A*B**, 10 mM sodium phosphate buffer pH 7.2, 0.1 mM spermine · 4 HCl, 20 resp. < 0.5 vol% ethanol.

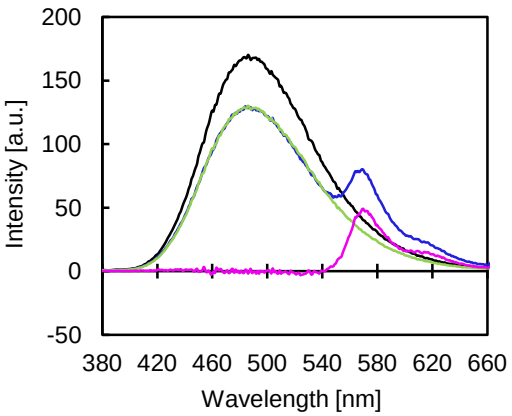

Fig. S36: Deconvolution of the fluorescence emission spectra before dialysis ($\lambda_{ex.}$: 335 nm). Undoped **A*B** (black), **A*B** + 1 mol% **E** (blue), deconvoluted TPE part of doped **A*B** (light green), deconvoluted Cy3 part of doped **A*B** (pink).

Table S5: Integrated fluorescence intensities for the calculation of the light-harvesting efficiency before dialysis. [a] Integration between 380–660 nm, $\lambda_{ex.}$: 335 nm.

	FL_{area} [a]
Undoped **A*B**	18891.4
A*B + 1 mol% Cy3	16777.4
TPE part of doped **A*B**	14732.6
Cy3 part of doped **A*B**	2044.8

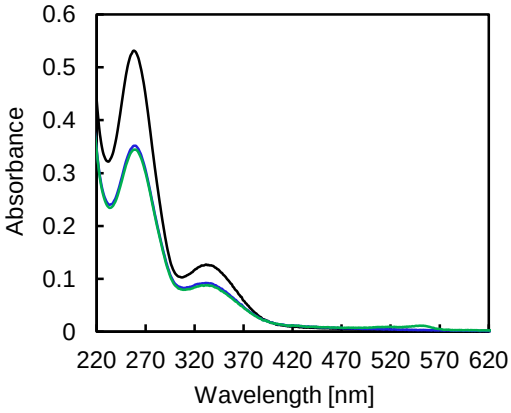

Fig. S37: UV-vis spectra of **A*B** (1 μM) in aqueous medium at 20 °C in the absence of **E** before (black, 20 vol% ethanol) and after (blue, < 0.5 vol% ethanol) dialysis and after dialysis in the presence of 1 mol% **E** (green, < 0.5 vol% ethanol).

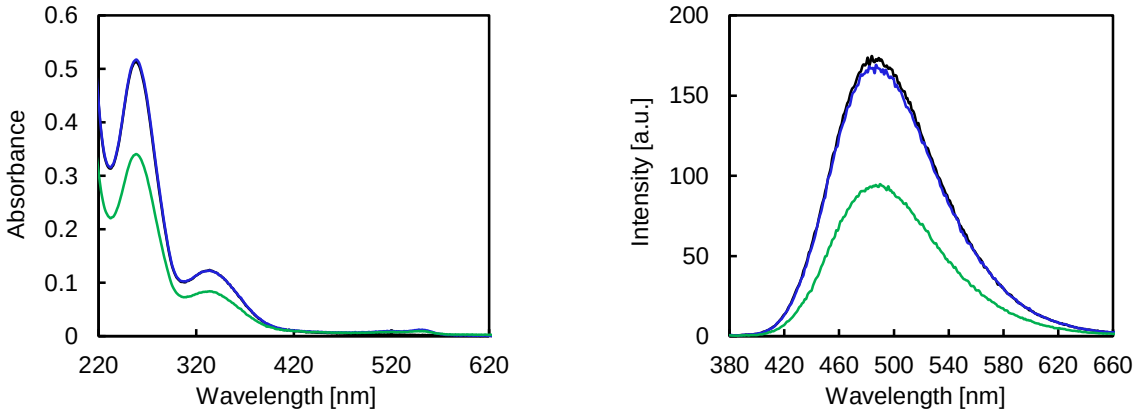

Fig. S38: UV-vis (left) and fluorescence emission spectra (right) of **A*B** in aqueous medium at 20 °C in the absence (black) and presence of 1 mol% **F** before (blue) and after (green) dialysis. Conditions: 1 μM **A*B**, 10 mM sodium phosphate buffer pH 7.2, 0.1 mM spermine · 4 HCl, 20 resp. < 0.5 vol% ethanol, $\lambda_{ex.}$: 335 nm.

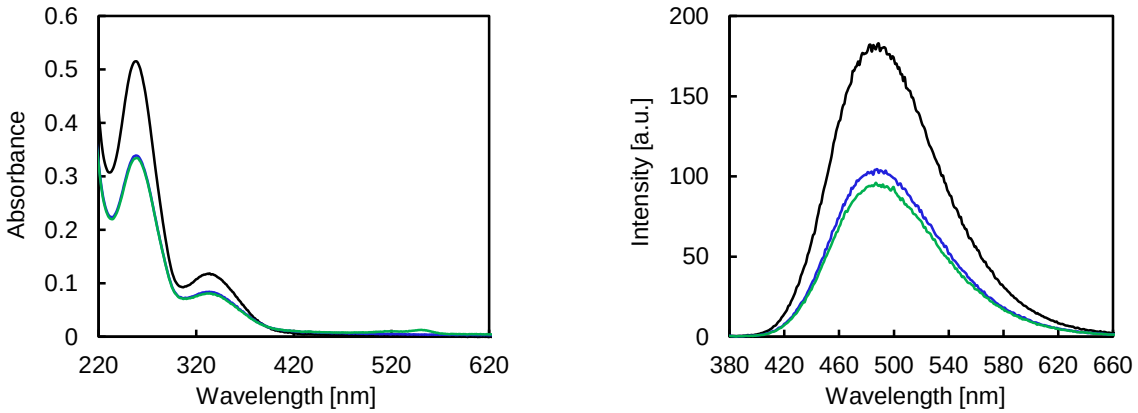

Fig. S39: UV-vis (left) and fluorescence emission spectra (right) of **A*B** (1 μM) in aqueous medium at 20 °C in the absence of **F** before (black, 20 vol% ethanol) and after (blue, < 0.5 vol% ethanol) dialysis and after dialysis in the presence of 1 mol% **F** (green, < 0.5 vol% ethanol), $\lambda_{ex.}$: 335 nm.

16. Bibliography

1 C. T. Rueden, J. Schindelin, M. C. Hiner, B. E. DeZonia, A. E. Walter, E. T. Arena and K. W. Eliceiri, *BMC Bioinformatics*, 2017, **18**, 529.

2 J. Schindelin, I. Arganda-Carreras, E. Frise, V. Kaynig, M. Longair, T. Pietzsch, S. Preibisch, C. Rueden, S. Saalfeld, B. Schmid, J.-Y. Tinevez, D. J. White, V. Hartenstein, K. Eliceiri, P. Tomancak and A. Cardona, *Nat. Methods*, 2012, **9**, 676–682.

3 M. Linkert, C. T. Rueden, C. Allan, J.-M. Burel, W. Moore, A. Patterson, B. Loranger, J. Moore, C. Neves, D. MacDonald, A. Tarkowska, C. Sticco, E. Hill, M. Rossner, K. W. Eliceiri and J. R. Swedlow, *J. Cell Biol.*, 2010, **189**, 777–782.

4 C. D. Bösch, S. M. Langenegger and R. Häner, *Angew. Chemie Int. Ed.*, 2016, **55**, 9961–9964.

5 S. Li, S. M. Langenegger and R. Häner, *Chem. Commun.*, 2013, **49**, 5835–5837.

6 S. Fery-Forgues and D. Lavabre, *J. Chem. Educ.*, 1999, **76**, 1260–1264.

7 W. H. Melhuish, *J. Phys. Chem.*, 1961, **65**, 229–235.

8 J. Cairns, *Cold Spring Harb. Symp. Quant. Biol.*, 1962, **27**, 311–318.